

1 **IL-33 induces an antiviral signature in mast cells but enhances their permissiveness for**  
2 **human rhinovirus infection**

3

4 Charlene Akoto <sup>1#</sup>, Anna Willis <sup>1#</sup>, Chiara F. Banas <sup>1#</sup>, Joseph A. Bell <sup>1</sup>, Dean Bryant <sup>2</sup>, Cornelia  
5 Blume <sup>3,4</sup>, Donna E. Davies <sup>1,4</sup> and Emily J. Swindle <sup>1,4,\*</sup>

6

7 <sup>1</sup>Clinical and Experimental Sciences, Faculty of Medicine, University of Southampton,  
8 University Hospital Southampton, Southampton, UK;

9 <sup>2</sup>Cancer Sciences, Faculty of Medicine, University of Southampton, University Hospital  
10 Southampton, Southampton, UK;

11 <sup>3</sup>Human Development and Health, Faculty of Medicine, University of Southampton,  
12 University Hospital Southampton, Southampton, UK;

13 <sup>3</sup>NIHR Southampton Biomedical Research Centre, University Hospital Southampton,  
14 Southampton, UK.

15 <sup>#</sup>Joint first authors

16 \*Corresponding author: Emily J. Swindle, e.j.swindle@soton.ac.uk

17

18 Key words: rhinovirus, infections, IL-33, mast cells

19

20 **Abstract**

21 Mast cells (MCs) are classically associated with allergic asthma but their role in antiviral  
22 immunity is unclear. Human rhinoviruses (HRVs) are a major cause of asthma exacerbations  
23 and can infect and replicate within MCs. The primary site of HRV infection is the airway  
24 epithelium and MCs localise to this site with increasing asthma severity. The asthma  
25 susceptibility gene, *IL-33*, encodes an epithelial-derived cytokine released following HRV  
26 infection but its impact on MC antiviral responses has yet to be determined. In this study we  
27 investigated the global response of LAD2 MCs to IL-33 stimulation using RNA sequencing  
28 and identified genes involved in antiviral immunity. In spite of this, IL-33 treatment increased  
29 permissiveness of MCs to HRV16 infection which, from the RNA-Seq data, we attributed to  
30 upregulation of ICAM1. Flow cytometric analysis confirmed an IL-33-dependent increase in  
31 ICAM1 surface expression as well as LDLR, the receptors used by major and minor group  
32 HRVs for cellular entry. Neutralisation of ICAM1 reduced the IL-33-dependent enhancement  
33 in HRV16 replication and release in both LAD2 MCs and cord blood derived MCs. These  
34 findings demonstrate that although IL-33 induces an antiviral signature in MCs, it also  
35 upregulates the receptors for HRV entry to enhance infection. This highlights the potential for  
36 a gene-environment interaction involving *IL33* and HRV in MCs to contribute to virus-induced  
37 asthma exacerbations.

38  
39  
40

41     **1. Introduction**

42     Mast cells (MCs) are tissue-resident immune cells that play important roles in innate and  
43     adaptive immunity. Their localisation within tissue enables them to form the first line of  
44     defence against invading pathogens, particularly parasites and bacteria [1]. However, in  
45     susceptible individuals, MCs are classically associated with the early phase reaction in allergic  
46     asthma [2, 3] in which specific allergens interact with IgE to cause Fc $\epsilon$ RI crosslinking on the  
47     surface of MCs leading to rapid release of mediators that cause bronchoconstriction. In asthma,  
48     MC numbers are increased in the bronchial epithelium, airway smooth muscle and submucosal  
49     glands and have an activated phenotype [4]. MC location and phenotype change with  
50     increasing asthma severity [5-7], are closely related to Th2 biomarkers [6] and MC activation  
51     is prominent in multidimensional clustering (MDS) of severe disease [8, 9]. Recent studies  
52     demonstrate that MC activation signatures are enriched across multiple clinical and molecular  
53     phenotypes of severe asthma [10] providing a strong association of MCs in asthma  
54     pathogenesis.

55

56     Due to their location at mucosal surfaces, MCs are important sentinel cells involved in  
57     immunity towards parasites and bacteria [1] but their role in antiviral immunity and virus-  
58     induced exacerbations are less well defined. MCs release interferons (IFNs) following toll-like  
59     receptor 3 (TLR3) activation, influenza A and respiratory syncytial virus (RSV) infection [11]  
60     and release chemokines and cytokines which recruit immune cells following infection with  
61     dengue virus or RSV [12-14]. While MCs can be infected with viruses and mount an immune  
62     response, they generally do not support replication of viruses, including RSV or influenza [14-  
63     16]. Human rhinoviruses (HRVs) are a major risk factor for asthma development in early life  
64     [17] and are the major cause of viral-induced exacerbations of asthma [18]. In a study of

65 experimental HRV infection, MC numbers were increased in the airways of asthmatic subjects  
66 and correlated with improved lung function during acute infection [19] suggesting MCs may  
67 play a protective role in virus-induced exacerbations of asthma. In contrast, treatment of  
68 asthmatic patients with the anti-IgE therapy omalizumab reduced MC numbers [20] and virus-  
69 induced exacerbations [21, 22] suggesting a harmful role for MCs in asthma exacerbations. We  
70 have previously shown that while MCs mount an innate immune response to HRV infection,  
71 they are permissive for viral replication and release infectious virus particles independent of  
72 cell death [23]. This is distinct amongst immune cells, which generally mount immune  
73 responses and do not release virus progeny [24-26]. While MCs appear to lack a robust type I  
74 IFN response to HRV infection, addition of exogenous IFN- $\beta$  protects them against infection  
75 [23].

76

77 Unbiased genome wide association studies (GWAS) have identified a large number of  
78 asthma susceptibility genes (and variants) that are expressed in the airway epithelium. These  
79 genes include *IL33* and its receptor *IL1RL1* (suppression of tumorigenicity 2 (ST2)) [27-30].  
80 The potential importance of the IL-33/ST2 axis in asthma is supported by several studies in  
81 which IL-33, ST2 and secretory ST2 (sST2) are increased in asthma compared to healthy  
82 controls and positively correlate with disease severity [31-35]. Furthermore, IL-33 enhances  
83 type 2 cytokine secretion by cells associated with asthma pathogenesis including MCs,  
84 basophils, T cells and type 2 innate lymphoid cells (ILC2s) [36, 37]. Due to its enhancing effect  
85 on type 2 cytokine secretion, approaches to neutralise IL-33 are currently being developed for  
86 asthma therapy [38] and have shown a reduction in exacerbation rates [39]. However, the role  
87 of IL-33 in innate immunity is not fully understood.

88 IL-33 is an alarmin with many roles including tissue homeostasis and repair, type 2  
89 inflammation and viral infections [40]. Depending on the type of viral infection IL-33 has either  
90 a protective or detrimental role and appears to be highly specific depending on the virus. For  
91 example, IL-33 is protective during choriomeningitis virus or herpes simplex virus infection  
92 while it exacerbates RSV and influenza virus-induced airway inflammation [41]. During  
93 experimental HRV infection, IL-33 is detected in the airways of asthmatic subjects and  
94 correlates with type 2 cytokine production, lower respiratory symptom scores and viral load  
95 [37]. In addition, *in vitro* HRV-infected bronchial epithelial cell (BEC) supernatants induced  
96 T cell and ILC2 type 2 cytokine release, which was suppressed following incubation with a  
97 ST2 blocking antibody suggesting that epithelial-derived IL-33 contributes to type 2  
98 inflammation [37]. While IL-33 enhances IgE-dependent MC responses and induces type 2  
99 cytokine secretion [42], its role in HRV-mediated MC responses is unknown.

100 In this study we investigated the global response of MCs to IL-33 stimulation and  
101 whether this has a functional consequence during viral infection. Following incubation of  
102 LAD2 MCs with IL-33, transcriptomic analysis revealed characteristic upregulation of type 2  
103 cytokine genes, as well as genes involved in antiviral immunity. However, when tested  
104 functionally, IL-33 treatment caused an unexpected increase in MC infection by HRV16; this  
105 was shown to be caused by an IL-33-dependent increase in intercellular adhesion molecule 1  
106 (ICAM-1), the cellular receptor used for HRV16, a major group rhinovirus. These effects were  
107 confirmed in both LAD2 MCs and cord blood derived MCs (CBMCs) and. The receptor used  
108 by minor group HRVs, low-density lipoprotein receptor (LDLR) was also upregulated by IL-  
109 33 treatment. The impact of IL-33 on MCs may have important consequences in viral-induced  
110 exacerbations of asthma: IL-33 release by a virally infected epithelium may predispose MCs  
111 for increased infectivity by HRV allowing MCs to contribute in a detrimental way to rhinovirus  
112 induced exacerbations of asthma.

113 **2. Materials and Methods**

114 Detailed methods can be found in Supplementary File S2.

115 *2.1. Mast cell culture*

116 The human MC line, LAD2, was obtained from Dr. A. Kirshenbaum (National  
117 Institutes of Health, Bethesda, USA) [43] and was cultured as previously described [23].  
118 Primary cord blood-derived MCs (CBMCs) were generated as previously described [23] from  
119 a commercial source of CD34+ cord blood progenitor cells (StemCell technologies, Grenoble,  
120 France).

121 *2.2. Rhinovirus stocks*

122 Human rhinovirus serotype 16 (HRV16, major group, HRV-B species) stocks were  
123 generated using H1-HeLa cells obtained from ATCC as previously described [23] and titres  
124 determined by tissue culture infective dose 50% (TCID<sub>50</sub>)/mL.

125 *2.3. Cell treatments and infections*

126 Human MCs (1x10<sup>6</sup>/ml) were incubated with IL-33 (1-10 ng/ml, R&D Systems,  
127 Abingdon, UK) for 6-24 hours in a humidified 37°C incubator with 5% CO<sub>2</sub> before  
128 transcriptomic and reverse transcription qPCR analyses. For HRV16 infection, MCs were pre-  
129 treated with IL-33 and then incubated with increasing multiplicity of infection (MOI: 1 – 7.5)  
130 of infectious virus or UV-irradiated virus (as a control) for 1 hour, washed twice then  
131 resuspended in StemPro media (0.5-1x10<sup>6</sup>/ml) for specified times before harvesting. For  
132 ICAM-1 blocking experiments, LAD2 MCs or CBMCs (1x10<sup>6</sup>/ml) were treated with 10 ng/ml  
133 IL-33 for 23 hours followed by 1 hour with mouse anti-human ICAM-1 (clone BBIG-I1  
134 (11C81), 10 µg/ml, R&D Systems, Abingdon, UK) or IgG2a isotype control (10 µg/ml, R&D

135 Systems, Abingdon, UK). Experimental layouts are shown in Supplementary File S2 (Figure  
136 A).

137 *2.4. mRNA extraction, RNA sequencing and transcriptomic analysis*

138 Total RNA was isolated using either the Trizol extraction method as previously  
139 described [23] or using commercially available kits (RNeasy minikit, Qiagen (Manchester,  
140 UK) or Monarch total RNA miniprep kit (New England Biolabs, Hitchin, UK)). Next  
141 generation sequencing was performed by Novogene (Cambridge, UK) before data processing  
142 and analysis as detailed in Supplementary File S2. Briefly, raw reads were mapped to the  
143 human genome (HISAT2), converted to counts (SAMtools) and adjusted for batch effects  
144 (ComBat Seq within sva package). After filtering out low counts (EdgER) remaining counts  
145 were normalised using a weighted trimmed mean of the log expression ratios (trimmed mean  
146 of M values (TMM)). The resultant expression matrix was used to create multidimensional  
147 scaling (MDS) plots (limma, Rstudio) and Heatmaps (heatmap.2, RStudio) and fitted to a  
148 generalised linear model (quasi-likelihood F-test) for differential expression. Differentially  
149 expressed genes (DEGs) were defined as genes with a log2(fold change) (log2FC)>1.5 and a  
150 False Discovery Rate (FDR)-adjusted p value <0.05. Upregulated genes were subjected to  
151 Gene ontology (GO) and pathways analysis (KEGG). Data are available at GSE216269.

152 *2.5. RT-qPCR*

153 cDNA template (12.5 ng) was used in quantitative PCR (qPCR) with Precision Plus  
154 double dye primers for housekeeping genes (HKGs; glyceraldehyde-3-phosphate  
155 dehydrogenase (*GAPDH*), ubiquitin C (*UBC*) or genes of interest (interferon induced with  
156 helicase C domain 1 (*IFIH1*), interferon regulatory factor 1 (*IRF1*), tumour necrosis factor  
157 alpha (*TNFA*), IFN beta 1 (*IFNBI*), IFN lambda 1 (*IFNL1*), 2',5'-oligoadenylate 1 (*OASI*), C-  
158 X-C motif chemokine ligand 10 (*CXCL10*), *IL6*, C-C motif chemokine ligand 5 (*CCL5*)) or

159 SYBR® green primers for genes of interest (*ICAM1*) used to quantify amplification of genes  
160 using a real-time PCR iCycler (BioRad, Hemel Hempstead, UK). Gene expression was  
161 normalised to the geometric means of HKGs and fold changes in gene expression calculated  
162 relative to UV-HRV16 controls according to the  $\Delta\Delta Ct$  method and expressed as  $2^{-\Delta\Delta Ct}$ . Viral  
163 RNA copy number was determined against a standard curve of known copies of HRV16  
164 (Primerdesign, Chandlers Ford, UK).

165 *2.6. Flow cytometry*

166 MCs ( $0.1 \times 10^6/100 \mu\text{l}$ ) were incubated with fluorescently labelled antibodies, FITC-  
167 conjugated mouse anti-human ICAM1 (clone RR1/1), subclass IgG<sub>1</sub>) or mouse IgG<sub>1</sub> isotype  
168 control (eBiosciences, Cheshire, UK) for 30 minutes with the addition of eBioscience™  
169 Fixable Viability Dye eFluor™ 660 (Thermo Fisher Scientific, Paisley, UK) on ice prior to  
170 resuspending in 300  $\mu\text{l}$  FACS buffer. Flow cytometry was performed using a BD FACSCalibur  
171 flow cytometer (BD Biosciences, Oxford, UK) and data analysed using FlowJo software  
172 (version 7.6.5, BD, Oregon, USA).

173 *2.7. TCID<sub>50</sub> assay*

174 The number of infectious virus particles in cell-free supernatants was determined by  
175 the TCID<sub>50</sub> assay where a 10-fold serial dilution of supernatants in quadruplicate were added  
176 to OHIO HeLa cells ( $0.2 \times 10^6/\text{well}$ , 96-well plate). After 96 hours, cytopathic effect (CPE) was  
177 visualised by staining monolayers with crystal violet solution (0.13% (w/v), 1.825% (v/v)  
178 formaldehyde, 5% ethanol (v/v), 90% PBS (v/v) for 30 minutes in the dark. Excess crystal  
179 violet was removed by gentle rinsing and the number of wells where at least 50% of the  
180 monolayer had been lysed (i.e. 50% CPE) was used to calculate TCID<sub>50</sub>/ml using the  
181 Spearman-Karber Method.

182 *2.8. Statistical analysis*

183 Paired non-parametric data were analysed by Wilcoxon signed rank test for matched  
184 pair comparisons. Un-paired non-parametric data were analysed by Kruskal–Wallis one-way  
185 ANOVA with Dunn's correction for multiple comparisons or Mann–Whitney ranked sum test  
186 and normalised data were analysed by Student's t-test. All data were analysed using GraphPad  
187 Prism (GraphPad Software, Inc., San Diego, CA, USA) and results were considered significant  
188 if  $p \leq 0.05$ , where \* $p \leq 0.05$ , \*\*  $p \leq 0.01$ , \*\*\*  $p \leq 0.001$ , \*\*\*\*  $p \leq 0.0001$ .

189

### 190 3. Results

#### 191 3.1. Transcriptomic analysis of MCs exposed to IL-33 reveals an antiviral gene signature

192 To determine the global response of LAD2 MCs following IL-33 stimulation, RNA-  
193 Seq was performed. Following 6h of treatment of MCs with IL-33, 414 differentially expressed  
194 genes (DEGs) ( $\log_2\text{FC} > 1.5$ , FDR-adjusted  $p < 0.05$ ) were identified (354 upregulated and 60  
195 downregulated) (Figure 1A). Hierarchical cluster analysis of DEGs identified 3 clusters that  
196 were upregulated in response to IL-33 treatment and two much smaller clusters that were down-  
197 regulated (Figure 1B). Of the top 100 most significantly DEGs, the majority were upregulated  
198 (Figure 1C). Further inspection of the top 50 DEGs (by  $\log_2\text{FC}$ ) identified genes known to be  
199 associated with IL-33 stimulation (e.g. cytokines such as *IL13*, *IL5*) (Table S1). However, this  
200 group also included genes encoding the virally induced gene Epstein-Barr Virus Induced 3  
201 (*EBI3*) and the viral-recognition gene (*TLR7*) (Table S1).

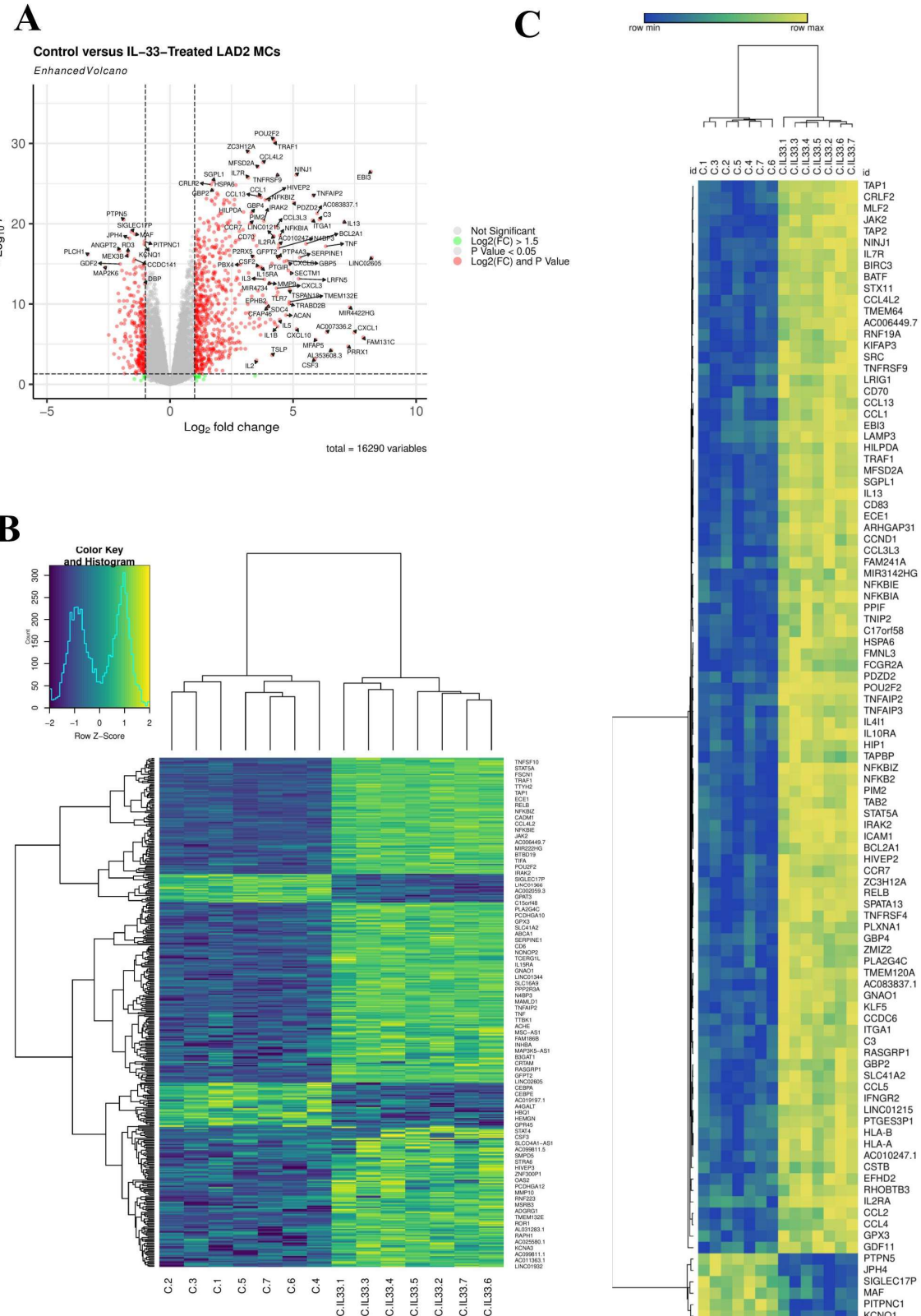


**Figure 1.** IL-33 induced 414 DEGs in MCs. **A**, volcano plot of DEGs 6h post IL-33 (10 ng/ml) treatment, n=7. **B**, Heatmap of all 414 DEGs 6h post IL-33 (10 ng/ml) treatment, N=7. **C**, Hierarchical clustering heatmap of top 100 most significant DEGs 6h post IL-33 (10 ng/ml)

203

204 Gene ontology (GO) analysis identified that IL-33 treated MCs were enriched for genes  
205 associated with *response to stimulus, regulation of response to stimulus, signaling, positive*  
206 *regulation of biological processes, cell adhesion and regulation of cell adhesion*, among many  
207 others (Figure 2A). When the list of GO processes significantly induced by IL-33 were ranked  
208 according to adjusted p value, genes associated with innate immunity including *defense*  
209 *response* (adj p value 4.81E-21) and *innate immune response* (adj p value 4.91E-07) were  
210 upregulated and more specifically genes associated with viral immunity including *response to*  
211 *virus* (adj p value 4.27E-05), *cellular response to virus* (adj p value 0.005), *negative regulation*  
212 *of viral genome replication* (adj p value 0.044) and *defense response to virus* (adj p value  
213 0.046). Kyoto Encyclopedia of Genes and Genomes (KEGG) pathway analysis identified in 35  
214 significantly upregulated pathways (Figure 2B). The top pathways associated with IL-33  
215 activation were, as expected, ‘*cytokine-cytokine receptor interactions*’, ‘*NF-kappa B signalling*  
216 *pathway*’ and ‘*TNF signalling pathway*’ and those associated with innate immunity (16 of 35).  
217 Amongst these pathways 7 of 16 were involved in anti-viral immunity (‘*viral protein*  
218 *interaction with cytokine and cytokine receptor*’, ‘*toll-like receptor signaling pathway*’,  
219 ‘*coronavirus disease – COVID-19*’, ‘*influenza A*’, ‘*measles*’, ‘*epstein-Barr virus infection*’, and  
220 ‘*human cytomegalovirus infection*’) (Figure 2B). Of particular interest was genes involved in  
221 the ‘*influenza A*’ pathway which included those involved in viral detection (*IFIH1*(MDA5),  
222 *OAS2* and *OAS3* (2-5’OAS), *TLR7*) and inflammation (*IL1B*, *CXCL8* (IL8), *IL33*, *TNFA*, *CCL2*  
223 (*MCP1*), *CCL5* (RANTES), *CXCL10* (IP-10)) (Figure 2C); further inspection of the DEGs also  
224 identified other antiviral genes associated with HRV infection. In total 24 antiviral genes were  
225 up-regulated by IL-33 (Figure S1) including *IFIH1*, and *TNFA* whose expression was  
226 confirmed by qPCR (Figure 2D). RTqPCR also demonstrated that induction of antiviral genes  
227 (*IFNB1*, *IFNL1*, *IFIH1*, *OAS1*, *CCL5*, *CXCL10*) occurred in an IL-33 concentration-dependent

228 manner and persisted for up to 24h (Figure S2). These data demonstrate that genes involved in  
 229 antiviral immunity are induced in MCs following IL-33 stimulation.

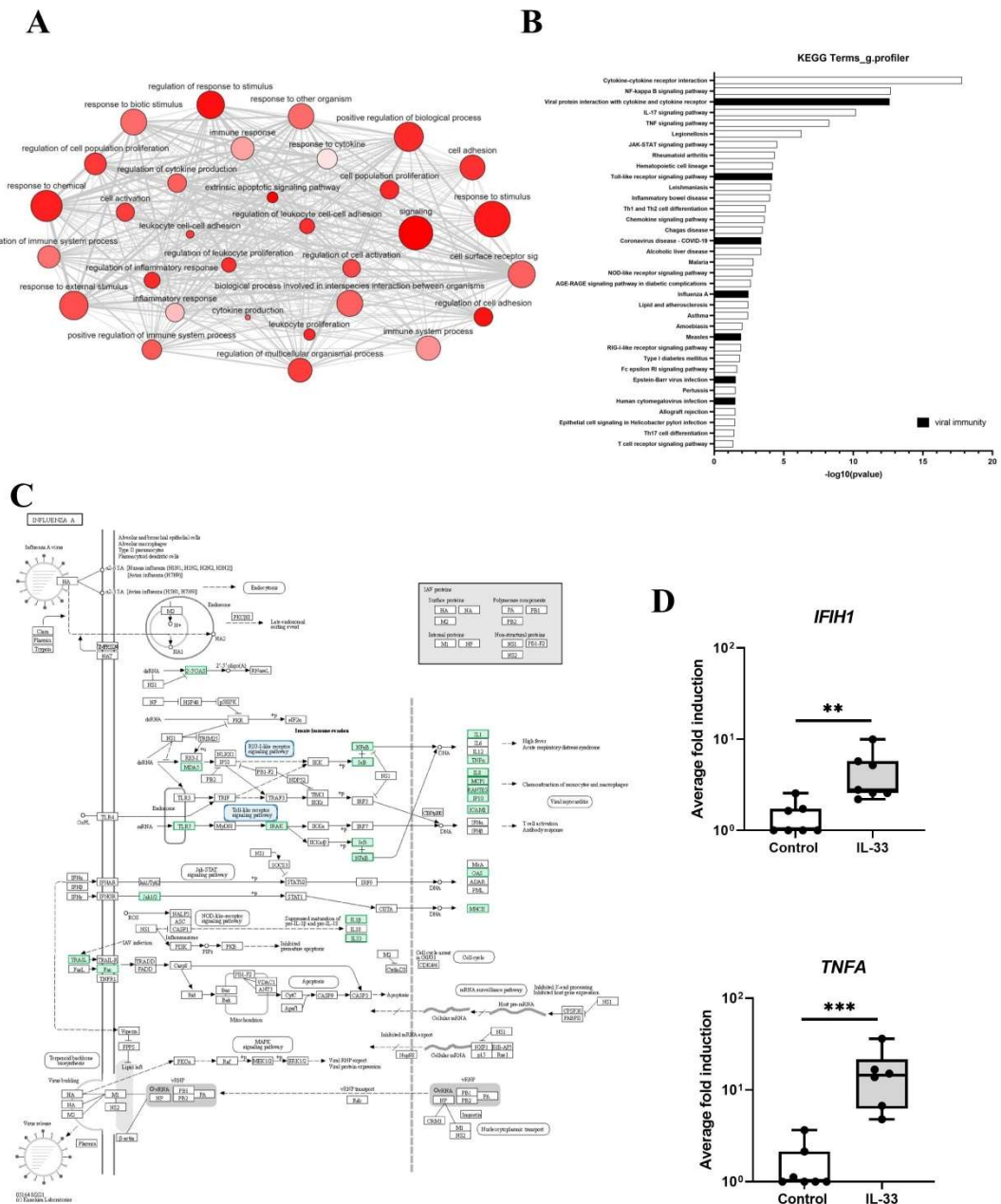


**Figure 2.** IL-33 induced DEGs associated with viral immunity in MCs. **A**, gene enrichment map of GO terms analysed using g.profiler. **B**, top KEGG pathways 6h post IL-33 (10 ng/ml) treatment, N=7. **C**, genes associated with the influenza Pathway using KEGG on DEGs 6h post IL-33 (10 ng/ml) treatment, N=7. **D**, mRNA expression of genes (*IFIH1*, *TNFA*) in influenza pathway 6h post IL-33 stimulation (10 ng/ml), N=7. \*\* $p\leq 0.01$ , \*\*\* $p\leq 0.001$  for control versus IL-33.

231

232 3.2. *IL-33 induces interferons and IFN-stimulated genes in LAD2 MCs*

233 To determine the functional consequence of the upregulation of antiviral genes in MCs  
234 by IL-33, LAD2 MCs were pre-treated with IL-33 (1-10 ng/ml) for 24h prior to infection with  
235 HRV16 (MOI 7.5) using UV-irradiated HRV16 as a control. Analysis of interferons (IFNs)  
236 and IFN stimulated genes (ISGs) 24h post-HRV16 infection revealed induction of *IFNB1* and  
237 *IFNL1* genes by HRV16 but not UV-HRV16 (Figure 3A-B). IL-33 concentration dependently  
238 increased *IFNB1* in the absence of infection while in the presence of both IL-33 and HRV16  
239 there was a further significant increase in expression of *IFNB1* and *IFNL1* (Figure 3A-B). A  
240 significant increase of HRV16-dependent secretion of IFN- $\beta$  protein in the presence of IL-33  
241 (10 ng/ml) was confirmed by ELISA (Figure 3E); no IFN- $\beta$  protein was detected in the UV-  
242 HRV16 control in the absence or presence of IL-33. There was also an IL-33 concentration-  
243 dependent increase in the gene expression of ISGs *IFIH1* and *OAS1* in the presence of HRV16  
244 (Figure 3C-D) suggesting that IL-33 enhanced antiviral immunity in MCs. Proinflammatory  
245 cytokine gene expression including *CXCL10* and *IL6* were similarly enhanced by IL-33 pre-  
246 treatment in both UV-HRV16 and HRV16 treated samples (Figure S3A&B) which was  
247 confirmed at the protein level for IL6 (Figure S3C). As anti-viral responses were greatest with  
248 10 ng/ml IL-33, the following experiments were conducted at this concentration.

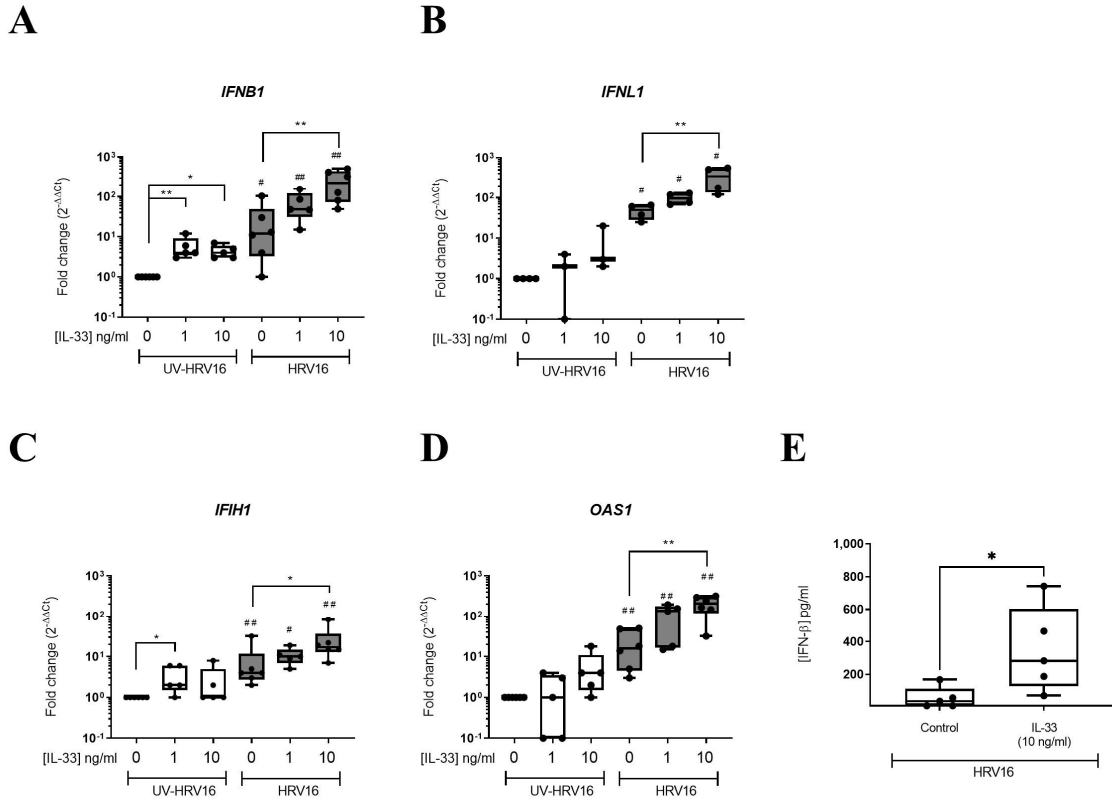


**Figure 3.** IL-33 enhanced HRV16-dependent anti-viral responses in MCs. mRNA expression of IFNs *IFNB1* (A), *IFNL1* (B) and IFN-stimulated genes *IFIH1* (C), *OAS1* (D) and IFN- $\beta$  protein (E) in LAD2 MCs pretreated with or without IL-33 (1-10 ng/ml) for 24h prior to HRV16 or UV-HRV16 (control) infection (MOI 7.5) for a further 24h, N=3-6. \* $p\leq 0.05$ , \*\* $p\leq 0.01$  for no cytokine versus IL-33 (1 or 10 ng/ml). # $p\leq 0.05$ , ## $p\leq 0.05$  for UV-HRV16 versus HRV16.

249

250

251 3.3. *IL-33 enhances HRV16 replication and release of infectious viral particles through*  
 252 *increased ICAM-1 expression*

253 In view of the enhanced anti-viral response mediated by IL-33, we next investigated  
 254 the impact of IL-33 on viral infection. LAD2 MCs were incubated with IL-33 for 24h prior to  
 255 HRV16 infection (MOI 7.5) for a further 24h. RT-qPCR for the viral genome showed IL-33  
 256 significantly increased HRV16 replication, which was paralleled by a significant rise in the  
 257 release of infectious virus particles as determined by TCID<sub>50</sub> assay (Figure 4A-B) suggesting  
 258 that rather than being protective, IL-33 promotes the infection of MCs by HRV16.

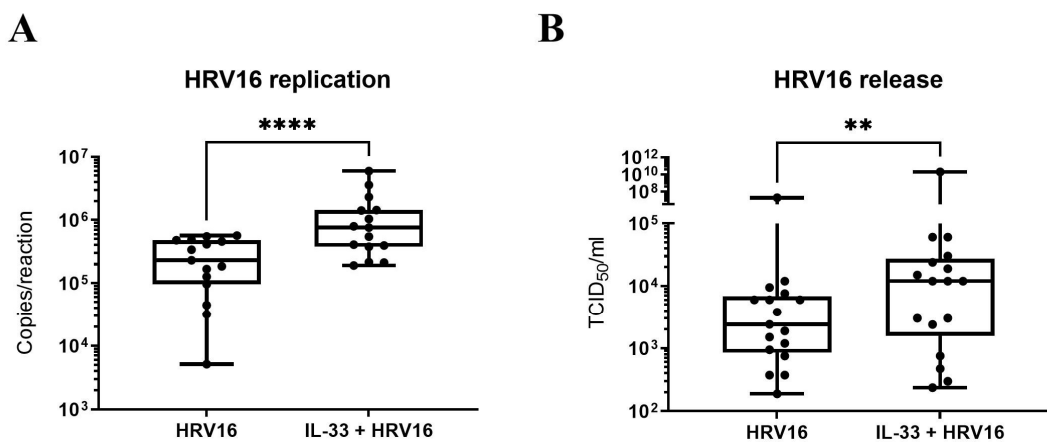


**Figure 4.** IL-33 enhances HRV16 replication and virion release in MCs. Viral RNA (A) and virion release (B) in LAD2 MCs pretreated with or without IL-33 (10 ng/ml) for 24h prior to HRV16 infection (MOI 7.5) for a further 24h, n=15. \*\* $p\leq 0.01$ , \*\*\*\* $p\leq 0.0001$  for HRV16 versus IL-33+HRV16.

Since IL-33 has been shown to increase expression of ICAM1, the receptor for major group HRVs, on endothelial cells [44] and murine MCs [45], we inspected the RNASeq data for expression of *ICAM1* and identified it within the DEGs (Figure S1). Flow cytometric analysis confirmed that IL-33 significantly increased the cell surface expression of ICAM1 (Figure 5A-B) after 24h incubation. While ICAM1 is the receptor for major group HRVs, minor group HRVs bind to the LDLR and HRVC binds to CDHR3. Therefore, we investigated the effect of IL-33 on expression of these receptors. By RTqPCR, we confirmed upregulation of *ICAM1* and found no effect of IL-33 on the low expression of *CDHR3* (control Ct 34.42±0.37) (Figure S4A&B), consistent with our previous study which reported that MCs do not express CDHR3 [23]. Flow cytometric analysis demonstrated the upregulation of LDLR cell surface expression by IL-33 (Figure S4C) on LAD2 MCs. IL-33 also upregulated its own receptor, membrane bound ST2 in LAD2 MCs (Figure S5A). To demonstrate that the increase in ICAM1 expression was responsible for the enhancement in HRV16 infection, MCs were pre-treated with IL-33 for 24h with and without an anti-ICAM1 antibody or isotype control

275 prior to HRV-16 infection for a further 24h. ICAM1 blockade significantly abrogated the IL-  
276 33-dependent increase in both HRV16 replication and release (Figure 5C-D) and this was  
277 paralleled by a significant drop in IL-33 enhanced IFN- $\beta$  release (Figure 5E). These data were  
278 confirmed in primary CBMCs which showed an IL-33-dependent increase in viral copy  
279 number (Figure 6A) and ICAM1 expression (Figure 6B-C), and that both HRV16 infection and  
280 IFN- $\beta$  release were abrogated by anti-ICAM1 blockade (Figure 6D-F). However, CBMCs were  
281 less responsive to IL-33 stimulation than LAD2 MCs which may be explained by their lower  
282 cell surface expression of ST2, the membrane bound receptor for IL-33 (Figure S5A-B). These  
283 data demonstrate that IL-33 increases the expression of ICAM-1 leading to enhanced  
284 replication and release of infectious virions in MCs.

285

286

287

288

289

290

291

292

293

294

295

296

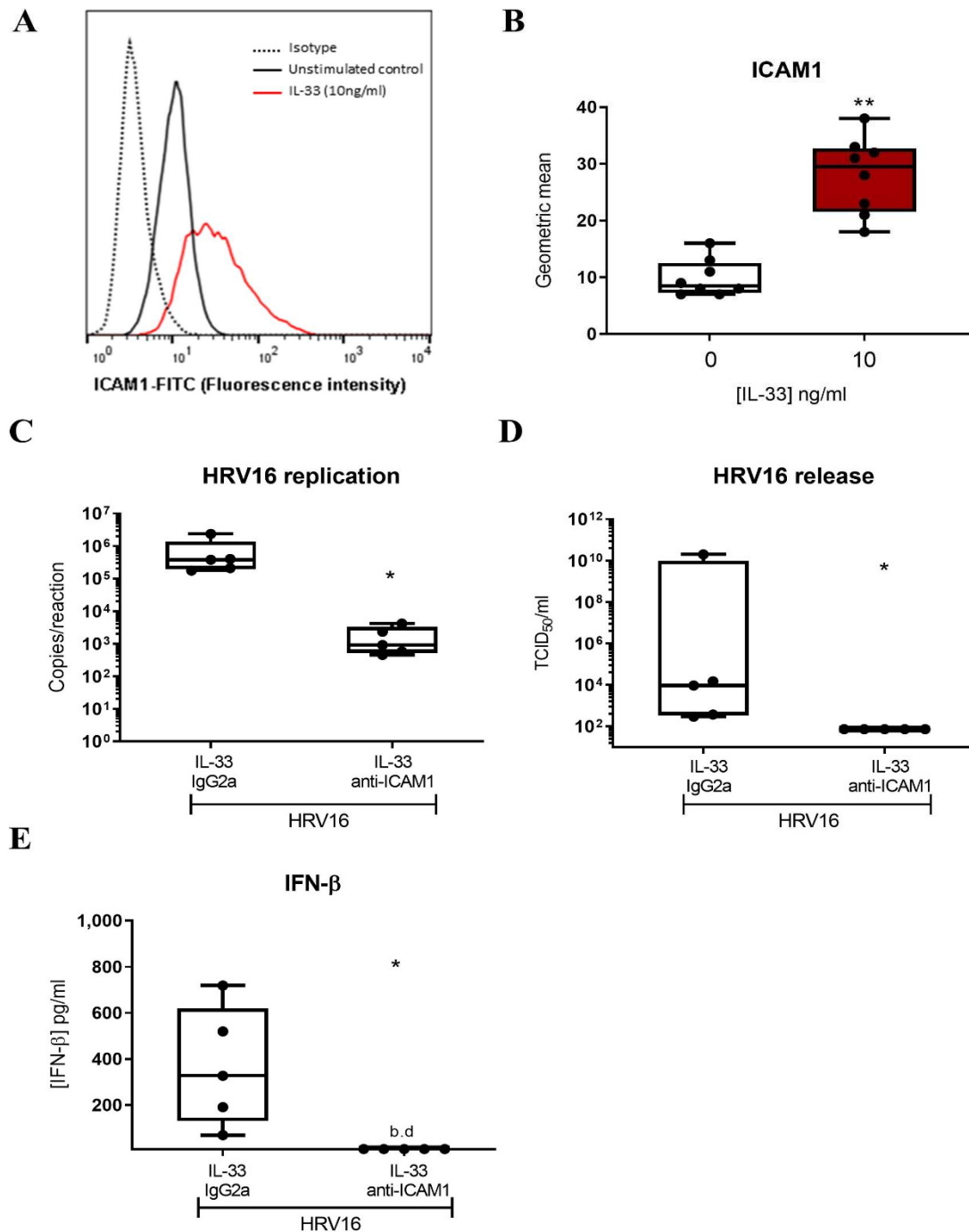


**Figure 5.** Role of ICAM1 in mediating IL-33-dependent enhancement of HRV16 replication in LAD2 MCs. A representative flow cytometric trace (A) and averaged geometric mean (B) for ICAM1 cell surface expression in MCs treated with IL-33 (10 ng/ml) for 24h, n=8. HRV16 replication (C) and virion release (D) and IFN- $\beta$  protein release (E) following IL-33 (10ng/ml) stimulation for 24h prior to HRV16 infection (MOI 7.5) in the presence or absence of anti-ICAM1 antibody or IgG2a isotype for a further 24h, n=5. \*\* $p\leq 0.01$  for no cytokine versus IL-33 and \* $p\leq 0.05$  for IL-33 IgG2a+HRV16 versus IL-33 anti-ICAM1+HRV16.

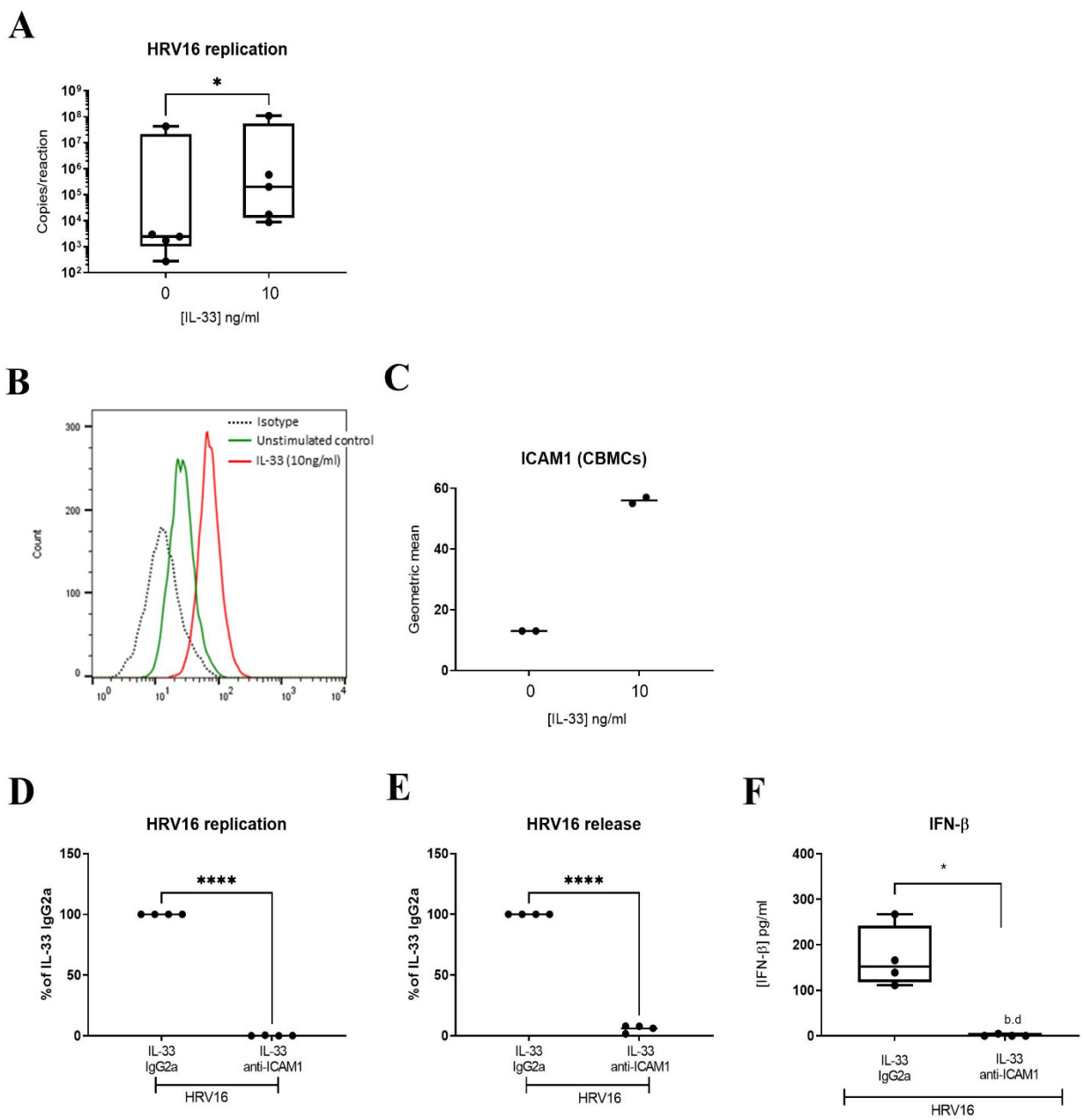


**Figure 6.** Role of ICAM1 in mediating IL-33-dependent enhancement of HRV16 replication in CBMCs. Viral RNA in CBMCs pretreated with or without IL-33 (10 ng/ml) for 24h prior to HRV16 infection (MOI 7.5) for a further 24h, n=5 (A). A representative flow cytometric trace (B) and averaged geometric mean (C) for ICAM1 cell surface expression in MCs treated with IL-33 (10 ng/ml) for 24h, n=2. HRV16 replication (D), virion release (E) and IFN- $\beta$  release (F) following IL-33 (10ng/ml) stimulation for 24h prior to HRV16 infection (MOI 7.5) in the presence or absence of anti-ICAM1 antibody or IgG2a isotype for a further 24h, n=4. \* $p\leq 0.05$  for no cytokine versus IL-33 and \* $p\leq 0.05$ , \*\* $p\leq 0.001$ , \*\*\* $p\leq 0.0001$  for IL-33 IgG2a+HRV16 versus IL-33 anti-ICAM1+HRV16.

299 **4. Discussion**

300 HRV infections are a major cause of asthma pathogenesis and exacerbation. MCs co-  
301 localise to the bronchial epithelium in asthma with increasing severity placing them at the main  
302 site for HRV replication and potentially contributing to HRV-induced exacerbations of asthma.  
303 *IL33* is an asthma susceptibility gene and IL-33 is released from the bronchial epithelium  
304 during HRV infection in asthmatic subjects. In this study we investigated the global response  
305 of MCs to IL-33 stimulation and determined whether this had a functional consequence during  
306 viral infection. We demonstrated that IL-33 induced an antiviral signature in MCs but rather  
307 than providing protection against HRV infection, IL-33 increased the infection of MC by HRV  
308 by causing upregulation in ICAM1, the receptor used by HRV16 for cellular entry. These data  
309 identify a potential gene-environment interaction involving the effect of IL-33 and HRV on  
310 MC that may have important consequences in virus-induced exacerbations of asthma.

311 During experimental HRV16 infection of allergic asthmatic subjects, an association  
312 was found between the number of subepithelial MCs and a lower maximum percent fall in  
313 peak expiratory flow (PEF) 4 days post-infection leading the authors to suggest that MCs are  
314 beneficial during HRV infection [19]. In contrast, anti-IgE therapy, which is known to reduce  
315 MC numbers [21], reduced asthma exacerbation rates [39] indicating that MCs play a  
316 detrimental role in virus-induced exacerbations of asthma. A major difference between these  
317 investigations was the severity of asthma studied; thus mild allergic asthmatics were used for  
318 the experimental infection studies [19], whereas the effect of anti-IgE therapy involved severe  
319 asthmatic subjects [21]. As MCs appear limited in their ability to produce sufficient Type I  
320 IFNs to protect against HRV infection [23], the selection of asthma patients may have an  
321 important influence on the outcome, since in mild asthma the epithelial antiviral Type I IFN  
322 response is greater than in severe disease [46] [47]. Thus, in mild asthma, the protection offered  
323 by epithelial-derived Type I IFNs towards MCs may outweigh the negative effect of IL-33 on

324 ICAM expression and viral entry whereas in severe disease, a lack of epithelial IFNs may  
325 render the MCs more vulnerable to infection. In support of this hypothesis, anti-ST2 therapy  
326 (astegolimab) reduces asthma exacerbation rates in severe asthmatic subjects.

327 In this paper we demonstrated that IL-33 induced an antiviral gene signature. While the  
328 focus of this paper was HRVs, MCs are also implicated in other respiratory viral infections  
329 including RSV and influenza. IL-33 is induced in the epithelium following RSV infection in  
330 asthmatic subjects [48] and infection of MCs with RSV causes an antiviral response suggesting  
331 they are beneficial in RSV-induced exacerbations of asthma. Since MCs do not support RSV  
332 replication, the influence of IL-33 in this setting might be expected to enhance antiviral  
333 immunity as any potential modulation of receptors used for entry by RSV, including  
334 ICAM1[49] would be unlikely to contribute to replication of the virus in MCs, although this  
335 remains to be determined experimentally. While IL-33 is increased in mice exposed to  
336 influenza A [50] and exogenous IL-33 is reported to protect against mucosal influenza A  
337 infection [51], its role in enhancing antiviral immunity and effects on MCs in this setting is yet  
338 to be determined.

339 Free IL-33 acts as a classical cytokine by binding to target cells expressing receptors  
340 for IL-33 consisting of ST2 and Interleukin-1 receptor accessory protein (IL-1RAcP) resulting  
341 in the formation of a stable dimer of the TIR-domains of ST2 and IL-1RAcP. The TIR-dimers  
342 are a scaffold for recruitment of a series of adaptor proteins, including the pivotal adaptor,  
343 MyD88, allowing activation of the classical MyD88/IRAK/TRAF6 module and downstream  
344 activation of NF- $\kappa$ B, stress-activated protein kinase p38 and c-Jun N-terminal kinases (JNK),  
345 as well as extracellularly regulated kinases (ERK1/2) and other signalling pathways [52]. The  
346 mechanism by which IL-33 induces antiviral immunity is yet to be determined. It may enhance  
347 Type I signalling via interleukin-1 receptor associated kinase 1/4 (IRAK1/4) and interferon

348 regulatory factor-3/7 pathways as these are key signalling factors in the production of Type I  
349 and III IFNs in BECs [53].

350 This paper is the first to describe the global response of human MCs to IL-33 using a  
351 transcriptomics approach. While Nagarkar *et al.* used gene expression microarrays to report  
352 the upregulation of cytokines, chemokines, and growth factors in IL-33 treated human  
353 peripheral blood derived MC [54], the entire dataset has not been made freely available.  
354 Related studies have been performed using mouse MCs where the global response of MCs to  
355 IgE-mediated activation was compared using bone marrow-derived MCs (BMMCs) from  
356 control and ST2 KO mice [55] This study demonstrated that the IL-33 activated transcriptome  
357 was enriched in genes commonly altered by NF- $\kappa$ B or in response to TNF, and a list of genes  
358 unique to IL-33 stimulation alone included some innate antiviral genes (*IRF5*, *CCL5*)  
359 suggesting some similarities with our human MC dataset.

360 IL-33 has variable effects on MCs depending on the length of exposure, concentration  
361 used and type of stimuli and typically induces MC adhesion, proliferation, maturation and  
362 activation and secretion of mediators [42]. Short term exposure enhances IgE-mediated  
363 degranulation, leukotriene and cytokine production [36, 56-58] while long term exposure  
364 (4wks) suppresses IgE-mediated degranulation via downregulation of hemopoietic cell kinase  
365 [59]. Furthermore, while high IL-33 concentrations (in the ng/ml range) induce cytokine  
366 secretion and enhance IgE-mediated activation, concentrations (in the pg/ml range) render MCs  
367 insensitive to bacterial cell wall components (LPS, PGN) [60]. In our studies, we tested IL-33  
368 at 1-10 ng/ml and found concentration-dependent effects on antiviral responses. Given their  
369 close proximity to epithelial cells in the airway of asthmatic subjects, it is possible that these  
370 concentrations may be achieved locally as a consequence of the cytopathic effect of HRVs on  
371 epithelial cells. Furthermore, other signals (e.g. allergen) present in the tissue

372 microenvironment may make important contributions to local IL-33 concentrations to  
373 influence MC contributions to viral-induced exacerbations of asthma.

374 In summary, we have shown that IL-33 induces an antiviral signature in MCs. In spite  
375 of this, when tested functionally this antiviral signature was insufficient to control HRV16  
376 replication as IL-33 increased expression of ICAM1 which facilitated infection and increased  
377 viral replication in MCs. Given that 60-80% of asthma exacerbations in adults and 90% of  
378 wheezing episodes in children [18, 61-63] are caused by HRVs, the impact of IL-33 to promote  
379 HRV infectivity of MCs may play an important role in the worsening of asthma symptoms. As  
380 *IL33* is an important asthma susceptibility gene, this effect of IL-33 on HRV infection of MCs  
381 highlights a potential gene-environment interaction that contributes to virus-induced asthma  
382 exacerbations.

383

384 **Supplementary Materials:** The following are available online at [www.mdpi.com/xxx/s1](http://www.mdpi.com/xxx/s1), Table S1:  
385 top 50 up- and down-regulated IL-33 induced DEGs in MCs, Figure S1: Violin plots of antiviral genes  
386 associated with HRV infection in LAD2 MCs, Figure S2: Concentration-dependent induction of IFN  
387 and IFN-inducible genes by IL-33 in MCs, Figure S3: RV16 affects IL-33-dependent CXCL10 and IL6  
388 release. Figure S4: IL-33 enhances ICAM1, LDLR but not CDHR3. Figure S5: IL-33 enhances  
389 membrane ST2 in LAD2 MCs and CBMCs. Supplementary file S1: Supplemental Figures.

390 **Author Contributions:** Conceptualization, E.J.S and D.E.D; methodology, C.A., C.F.B. and A.W.;  
391 software, C.F.B. A.W. D.B. and J.A.B.; validation, C.A., C.F.B., A.W., C.B., J.A.B., D.E.D and E.J.S.;  
392 formal analysis, C.A., C.F.B., A.W. and E.J.S.; investigation, C.A., C.F.B. and A.W.; resources, D.E.D.  
393 and E.J.S.; data curation, C.A., C.F.B., A.W., D.B. and J.A.B.; writing—original draft preparation,  
394 E.J.S.; writing—review and editing, D.E.D., C.B. and E.J.S.; visualization, C.A., C.F.B., A.W and  
395 E.J.S.; supervision, E.J.S. D.E.D., C.B.; project administration, E.J.S.; funding acquisition, E.J.S. All  
396 authors have read and agreed to the published version of the manuscript.

397 **Funding:** This research was funded by the MRC DTP programme award to the Faculty of Medicine,  
398 University of Southampton (grant number MR/N014308/1), the Asthma, Allergy and Inflammation  
399 Research (AAIR) Charity and the Faculty of Medicine, University of Southampton. The APC was  
400 funded by MR/N014308/1.

401 **Institutional Review Board Statement:** Not applicable.

402 **Informed Consent Statement:** Not applicable.

403 **Data Availability Statement:** The data that support the findings of this study are openly available in  
404 the University of Southampton repository at <https://doi.org/10.5258/SOTON/D2415> and transcriptomic  
405 data accession number GSE216269.

406 **Acknowledgments:** We thank Arnold Kirschenbaum and Dean D. Metcalfe (NIH) for the initial gift  
407 of LAD2 MCs, which were used in this study. We also thank Mark Lennon (Biostatistics, GSK) and  
408 Wendy Rowan for their assistance in determining the number of replicate experiments to perform for  
409 RNA-Seq.

410 **Conflicts of Interest:** Professor Donna Davies is a cofounder of Synairgen and is paid consultancy fees  
411 and also has a patent for the use of inhaled interferon beta therapy for virus-induced exacerbations of  
412 asthma and COPD with royalties paid.

413

## 414 **References**

- 415 1. Abraham SN, St John AL. Mast cell-orchestrated immunity to pathogens. *Nat Rev Immunol.* 2010;10(6):440-52.
- 416 2. Metcalfe DD, Baram D, Mekori YA. Mast cells. *Physiol Rev.* 1997;77(4):1033-79.
- 417 3. Bradding P, Arthur G. Mast cells in asthma--state of the art. *Clin Exp Allergy.* 2016;46(2):194-263.
- 418 4. Bradding P, Walls AF, Holgate ST. The role of the mast cell in the pathophysiology of  
419 asthma. *J Allergy Clin Immunol.* 2006;117(6):1277-84.
- 420 5. Andersson CK, Bergqvist A, Mori M, Mauad T, Bjermer L, Erjefalt JS. Mast cell-  
421 associated alveolar inflammation in patients with atopic uncontrolled asthma. *J Allergy Clin  
422 Immunol.* 2011;127(4):905-12 e1-7.

425 6. Dougherty RH, Sidhu SS, Raman K, Solon M, Solberg OD, Caughey GH, et al.  
426 Accumulation of intraepithelial mast cells with a unique protease phenotype in T(H)2-high  
427 asthma. *J Allergy Clin Immunol.* 2010;125(5):1046-53 e8.

428 7. Balzar S, Fajt ML, Comhair SA, Erzurum SC, Bleeker E, Busse WW, et al. Mast cell  
429 phenotype, location, and activation in severe asthma. Data from the Severe Asthma Research  
430 Program. *Am J Respir Crit Care Med.* 2010;183(3):299-309.

431 8. Hinks T, Zhou X, Staples K, Dimitrov B, Manta A, Petrossian T, et al. Multidimensional endotypes of asthma: topological data analysis of cross-sectional clinical,  
432 pathological, and immunological data. *Lancet.* 2015;385 Suppl 1:S42.

433 9. Hinks TS, Zhou X, Staples KJ, Dimitrov BD, Manta A, Petrossian T, et al. Innate and  
434 adaptive T cells in asthmatic patients: Relationship to severity and disease mechanisms. *J*  
435 *Allergy Clin Immunol.* 2015;136(2):323-33.

436 10. Tiotiu A, Badi Y, Kermani NZ, Sanak M, Kolmert J, Wheelock CE, et al. Association  
437 of Differential Mast Cell Activation with Granulocytic Inflammation in Severe Asthma. *Am J*  
438 *Respir Crit Care Med.* 2022;205(4):397-411.

439 11. Kulka M, Alexopoulou L, Flavell RA, Metcalfe DD. Activation of mast cells by double-  
440 stranded RNA: evidence for activation through Toll-like receptor 3. *J Allergy Clin Immunol.*  
441 2004;114(1):174-82.

442 12. Burke SM, Issekutz TB, Mohan K, Lee PW, Shmulevitz M, Marshall JS. Human mast  
443 cell activation with virus-associated stimuli leads to the selective chemotaxis of natural killer  
444 cells by a CXCL8-dependent mechanism. *Blood.* 2008;111(12):5467-76.

445 13. McAlpine SM, Issekutz TB, Marshall JS. Virus stimulation of human mast cells results  
446 in the recruitment of CD56+ T cells by a mechanism dependent on CCR5 ligands. *FASEB J.*  
447 2011;26(3):1280-9.

448 14. Al-Afif A, Alyazidi R, Oldford SA, Huang YY, King CA, Marr N, et al. Respiratory  
449 syncytial virus infection of primary human mast cells induces the selective production of type  
450 I interferons, CXCL10, and CCL4. *J Allergy Clin Immunol.* 2015;136(5):1346-54 e1.

451 15. Shirato K, Taguchi F. Mast cell degranulation is induced by A549 airway epithelial cell  
452 infected with respiratory syncytial virus. *Virology.* 2009;386(1):88-93.

453 16. Ng K, Raheem J, St Laurent CD, Marcket CT, Vliagostis H, Befus AD, et al. Responses  
454 of human mast cells and epithelial cells following exposure to influenza A virus. *Antiviral Res.*  
455 2019;171:104566.

456 17. Jackson DJ, Gangnon RE, Evans MD, Roberg KA, Anderson EL, Pappas TE, et al.  
457 Wheezing rhinovirus illnesses in early life predict asthma development in high-risk children.  
458 *Am J Respir Crit Care Med.* 2008;178(7):667-72.

459 18. Johnston SL, Pattemore PK, Sanderson G, Smith S, Lampe F, Josephs L, et al.  
460 Community study of role of viral infections in exacerbations of asthma in 9-11 year old  
461 children. *Bmj.* 1995;310(6989):1225-9.

462 19. Zhu J, Message SD, Qiu Y, Mallia P, Kebadze T, Contoli M, et al. Airway inflammation  
463 and illness severity in response to experimental rhinovirus infection in asthma. *Chest.* 2014.

464 20. Djukanovic R, Wilson SJ, Kraft M, Jarjour NN, Steel M, Chung KF, et al. Effects of  
465 treatment with anti-immunoglobulin E antibody omalizumab on airway inflammation in  
466 allergic asthma. *Am J Respir Crit Care Med.* 2004;170(6):583-93.

467 21. Brusselle G, Michils A, Louis R, Dupont L, Van de Maele B, Delobbe A, et al. "Real-  
468 life" effectiveness of omalizumab in patients with severe persistent allergic asthma: The  
469 PERSIST study. *Respir Med.* 2009;103(11):1633-42.

470 22. Soler M, Matz J, Townley R, Buhl R, O'Brien J, Fox H, et al. The anti-IgE antibody  
471 omalizumab reduces exacerbations and steroid requirement in allergic asthmatics. *Eur Respir*  
472 *J.* 2001;18(2):254-61.

473

474 23. Akoto C, Davies DE, Swindle EJ. Mast cells are permissive for rhinovirus replication:  
475 potential implications for asthma exacerbations. *Clin Exp Allergy*. 2017;47(3):351-60.

476 24. Schrauf C, Kirchberger S, Majdic O, Seyerl M, Zlabinger GJ, Stuhlmeier KM, et al.  
477 The ssRNA genome of human rhinovirus induces a type I IFN response but fails to induce  
478 maturation in human monocyte-derived dendritic cells. *J Immunol*. 2009;183(7):4440-8.

479 25. Gern JE, Vrtis R, Kelly EA, Dick EC, Busse WW. Rhinovirus produces nonspecific  
480 activation of lymphocytes through a monocyte-dependent mechanism. *J Immunol*.  
481 1996;157(4):1605-12.

482 26. Laza-Stanca V, Stanciu LA, Message SD, Edwards MR, Gern JE, Johnston SL.  
483 Rhinovirus replication in human macrophages induces NF-kappaB-dependent tumor necrosis  
484 factor alpha production. *J Virol*. 2006;80(16):8248-58.

485 27. Moffatt MF, Gut IG, Demenais F, Strachan DP, Bouzigon E, Heath S, et al. A large-  
486 scale, consortium-based genomewide association study of asthma. *N Engl J Med*.  
487 2010;363(13):1211-21.

488 28. Torgerson DG, Ampleford EJ, Chiu GY, Gauderman WJ, Gignoux CR, Graves PE, et  
489 al. Meta-analysis of genome-wide association studies of asthma in ethnically diverse North  
490 American populations. *Nat Genet*. 2011;43(9):887-92.

491 29. Ramasamy A, Kuokkanen M, Vedantam S, Gajdos ZK, Couto Alves A, Lyon HN, et  
492 al. Genome-wide association studies of asthma in population-based cohorts confirm known  
493 and suggested loci and identify an additional association near HLA. *PLoS One*.  
494 2012;7(9):e44008.

495 30. Portelli MA, Dijk FN, Ketelaar ME, Shrine N, Hankinson J, Bhaker S, et al. Phenotypic  
496 and functional translation of IL1RL1 locus polymorphisms in lung tissue and asthmatic airway  
497 epithelium. *JCI Insight*. 2020;5(8).

498 31. Prefontaine D, Lajoie-Kadoch S, Foley S, Audusseau S, Olivenstein R, Halayko AJ, et  
499 al. Increased expression of IL-33 in severe asthma: evidence of expression by airway smooth  
500 muscle cells. *J Immunol*. 2009;183(8):5094-103.

501 32. Prefontaine D, Nadigel J, Chouiali F, Audusseau S, Semlali A, Chakir J, et al. Increased  
502 IL-33 expression by epithelial cells in bronchial asthma. *J Allergy Clin Immunol*.  
503 2010;125(3):752-4.

504 33. Saglani S, Lui S, Ullmann N, Campbell GA, Sherburn RT, Mathie SA, et al. IL-33  
505 promotes airway remodeling in pediatric patients with severe steroid-resistant asthma. *J  
506 Allergy Clin Immunol*. 2013;132(3):676-85 e13.

507 34. Traister RS, Uvalle CE, Hawkins GA, Meyers DA, Bleecker ER, Wenzel SE.  
508 Phenotypic and genotypic association of epithelial IL1RL1 to human TH2-like asthma. *J  
509 Allergy Clin Immunol*. 2015;135(1):92-9.

510 35. Gordon ED, Simpson LJ, Rios CL, Ringel L, Lachowicz-Scroggins ME, Peters MC, et  
511 al. Alternative splicing of interleukin-33 and type 2 inflammation in asthma. *Proc Natl Acad  
512 Sci U S A*. 2016;113(31):8765-70.

513 36. Allakhverdi Z, Smith DE, Comeau MR, Delespesse G. Cutting edge: The ST2 ligand  
514 IL-33 potently activates and drives maturation of human mast cells. *J Immunol*.  
515 2007;179(4):2051-4.

516 37. Jackson DJ, Makrinioti H, Rana BM, Shamji BW, Trujillo-Torralbo MB, Footitt J, et  
517 al. IL-33-dependent type 2 inflammation during rhinovirus-induced asthma exacerbations in  
518 vivo. *Am J Respir Crit Care Med*. 2014;190(12):1373-82.

519 38. Wechsler ME, Ruddy MK, Pavord ID, Israel E, Rabe KF, Ford LB, et al. Efficacy and  
520 Safety of Itepekimab in Patients with Moderate-to-Severe Asthma. *N Engl J Med*.  
521 2021;385(18):1656-68.

522 39. Kelsen SG, Agache IO, Soong W, Israel E, Chupp GL, Cheung DS, et al. Astegolimab  
523 (anti-ST2) efficacy and safety in adults with severe asthma: A randomized clinical trial. *J*  
524 *Allergy Clin Immunol.* 2021;148(3):790-8.

525 40. Cayrol C, Girard JP. Interleukin-33 (IL-33): A critical review of its biology and the  
526 mechanisms involved in its release as a potent extracellular cytokine. *Cytokine.*  
527 2022;156:155891.

528 41. Liew FY, Girard JP, Turnquist HR. Interleukin-33 in health and disease. *Nat Rev*  
529 *Immunol.* 2016;16(11):676-89.

530 42. Saluja R, Zoltowska A, Ketelaar ME, Nilsson G. IL-33 and Thymic Stromal  
531 Lymphopoietin in mast cell functions. *Eur J Pharmacol.* 2016;778:68-76.

532 43. Kirshenbaum AS, Akin C, Wu Y, Rottem M, Goff JP, Beaven MA, et al. Characterization of novel stem cell factor responsive human mast cell lines LAD 1 and 2  
533 established from a patient with mast cell sarcoma/leukemia; activation following aggregation  
534 of FcepsilonRI or FcgammaRI. *Leuk Res.* 2003;27(8):677-82.

536 44. Gautier V, Cayrol C, Farache D, Roga S, Monsarrat B, Burlet-Schiltz O, et al. Extracellular IL-33 cytokine, but not endogenous nuclear IL-33, regulates protein expression  
537 in endothelial cells. *Sci Rep.* 2016;6:34255.

539 45. Numata T, Ito T, Maeda T, Egusa C, Tsuboi R. IL-33 promotes ICAM-1 expression via  
540 NF- $\kappa$ B in murine mast cells. *Allergol Int.* 2016;65(2):158-65.

541 46. Farne H, Lin L, Jackson DJ, Rattray M, Simpson A, Custovic A, et al. In vivo bronchial  
542 epithelial interferon responses are augmented in asthma on day 4 following experimental  
543 rhinovirus infection. *Thorax.* 2022;77(9):929-32.

544 47. Wark PA, Johnston SL, Buccieri F, Powell R, Puddicombe S, Laza-Stanca V, et al. Asthmatic bronchial epithelial cells have a deficient innate immune response to infection with  
545 rhinovirus. *J Exp Med.* 2005;201(6):937-47.

547 48. Andersson CK, Iwasaki J, Cook J, Robinson P, Nagakumar P, Mogren S, et al. Impaired  
548 airway epithelial cell wound-healing capacity is associated with airway remodelling following  
549 RSV infection in severe preschool wheeze. *Allergy.* 2020;75(12):3195-207.

550 49. Battles MB, McLellan JS. Respiratory syncytial virus entry and how to block it. *Nat*  
551 *Rev Microbiol.* 2019;17(4):233-45.

552 50. Le Goffic R, Arshad MI, Rauch M, L'Helgoualc'h A, Delmas B, Piquet-Pellorce C, et  
553 al. Infection with influenza virus induces IL-33 in murine lungs. *Am J Respir Cell Mol Biol.*  
554 2011;45(6):1125-32.

555 51. Kim CW, Yoo HJ, Park JH, Oh JE, Lee HK. Exogenous Interleukin-33 Contributes to  
556 Protective Immunity via Cytotoxic T-Cell Priming against Mucosal Influenza Viral Infection.  
557 *Viruses.* 2019;11(9).

558 52. Martin MU. Special aspects of interleukin-33 and the IL-33 receptor complex. *Semin*  
559 *Immunol.* 2013;25(6):449-57.

560 53. Gavala ML, Bertics PJ, Gern JE. Rhinoviruses, allergic inflammation, and asthma.  
561 *Immunol Rev.* 2011;242(1):69-90.

562 54. Nagarkar DR, Ramirez-Carrozzi V, Choy DF, Lee K, Soriano R, Jia G, et al. IL-13  
563 mediates IL-33-dependent mast cell and type 2 innate lymphoid cell effects on bronchial  
564 epithelial cells. *J Allergy Clin Immunol.* 2015;136(1):202-5.

565 55. Chhiba KD, Hsu CL, Berdnikovs S, Bryce PJ. Transcriptional Heterogeneity of Mast  
566 Cells and Basophils upon Activation. *J Immunol.* 2017;198(12):4868-78.

567 56. Iikura M, Suto H, Kajiwara N, Oboki K, Ohno T, Okayama Y, et al. IL-33 can promote  
568 survival, adhesion and cytokine production in human mast cells. *Lab Invest.* 2007;87(10):971-  
569 8.

570 57. Silver MR, Margulis A, Wood N, Goldman SJ, Kasaian M, Chaudhary D. IL-33  
571 synergizes with IgE-dependent and IgE-independent agents to promote mast cell and basophil  
572 activation. *Inflamm Res.* 2010;59(3):207-18.

573 58. Andrade MV, Iwaki S, Ropert C, Gazzinelli RT, Cunha-Melo JR, Beaven MA.  
574 Amplification of cytokine production through synergistic activation of NFAT and AP-1  
575 following stimulation of mast cells with antigen and IL-33. *Eur J Immunol.* 2011;41(3):760-  
576 72.

577 59. Jung MY, Smrz D, Desai A, Bandara G, Ito T, Iwaki S, et al. IL-33 induces a  
578 hyporesponsive phenotype in human and mouse mast cells. *J Immunol.* 2013;190(2):531-8.

579 60. Sandig H, Jobbings CE, Roldan NG, Whittingham-Dowd JK, Orinska Z, Takeuchi O,  
580 et al. IL-33 causes selective mast cell tolerance to bacterial cell wall products by inducing  
581 IRAK1 degradation. *Eur J Immunol.* 2013;43(4):979-88.

582 61. Turunen R, Koistinen A, Vuorinen T, Arku B, Soderlund-Venermo M, Ruuskanen O,  
583 et al. The first wheezing episode: respiratory virus etiology, atopic characteristics, and illness  
584 severity. *Pediatr Allergy Immunol.* 2014;25(8):796-803.

585 62. Grissell TV, Powell H, Shafren DR, Boyle MJ, Hensley MJ, Jones PD, et al.  
586 Interleukin-10 gene expression in acute virus-induced asthma. *Am J Respir Crit Care Med.*  
587 2005;172(4):433-9.

588 63. Papadopoulos NG, Christodoulou I, Rohde G, Agache I, Almqvist C, Bruno A, et al.  
589 Viruses and bacteria in acute asthma exacerbations--a GA(2) LEN-DARE systematic review.  
590 *Allergy.* 2011;66(4):458-68.

591

592

593 **Supplementary File S1: Supplemental Figures**

594 **Table S1:** Top 50 upregulated and downregulated genes in IL-33-activated MCs compared to control  
 595 samples. Genes were ranked by fold change and the top 50 upregulated and downregulated genes were  
 596 taken. Genes in bold were antiviral genes identified through KEGG pathway analysis.

597

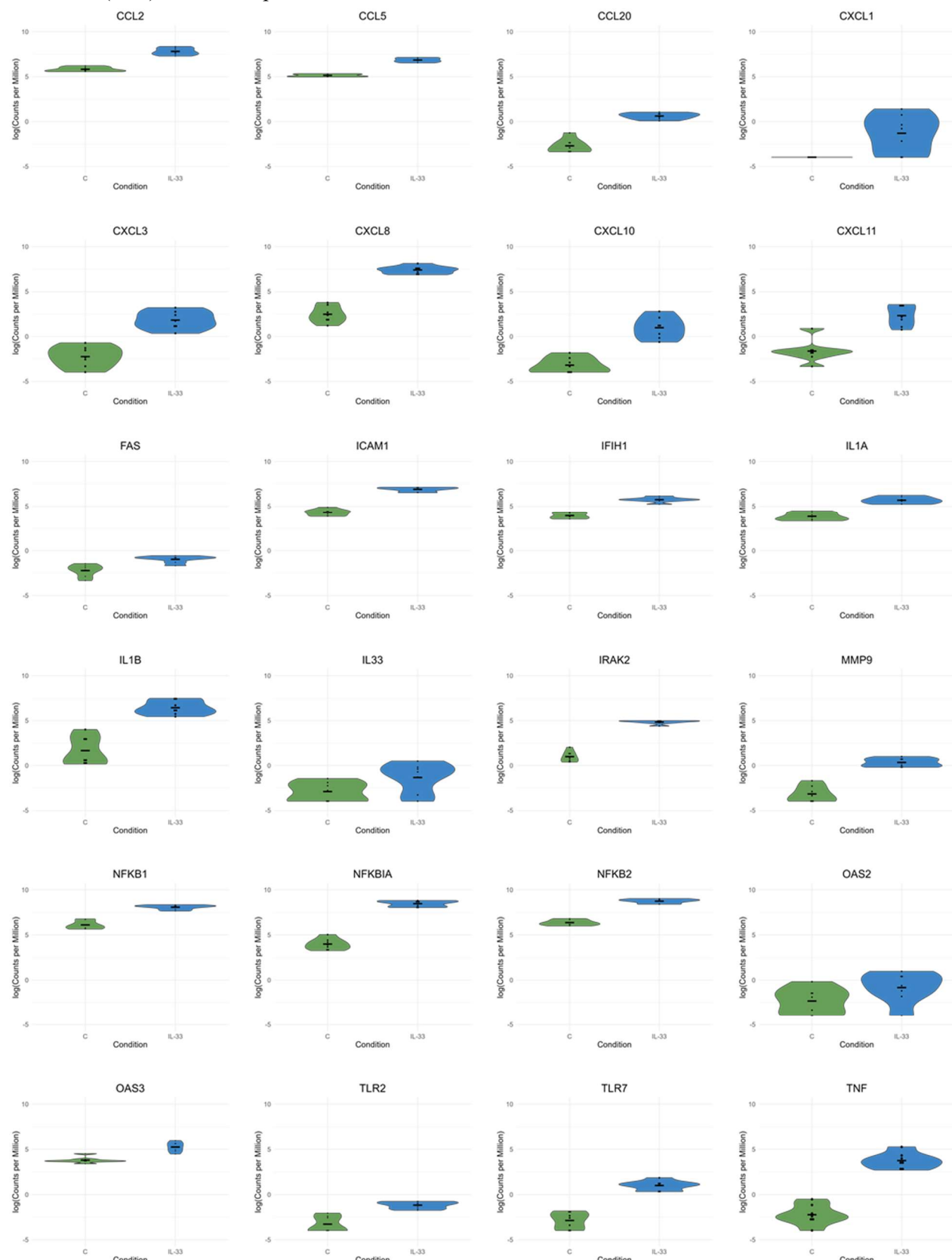
Top 50 upregulated genes in C vs C+IL33 by FC					Top 50 downregulated genes in C vs C+IL33 by FC				
	Gene	FDR	FC	log <sub>2</sub> FC		Gene	FDR	FC	log <sub>2</sub> FC
1	<i>LINC02605</i>	1.82E-14	295.50	8.207	1	<i>PLCH1</i>	7.86E-15	-10.07	-3.33
2	<b><i>EBI3</i></b>	<b>8.94E-24</b>	<b>287.02</b>	<b>8.165</b>	2	<i>MAP2K6</i>	2.30E-13	-6.21	-2.63
3	<i>FAM131C</i>	1.54E-05	230.56	7.849	3	<i>ARHGEF4</i>	8.44E-06	-5.63	-2.49
4	<i>CXCL1</i>	4.54E-06	179.02	7.484	4	<i>TBXA2R</i>	0.001059	-4.84	-2.28
5	<i>MIR4422HG</i>	7.02E-09	157.26	7.297	5	<i>HBQ1</i>	2.57E-05	-4.75	-2.25
6	<i>PRRX1</i>	0.000152	150.44	7.233	6	<i>SCN2A</i>	4.85E-05	-4.73	-2.24
7	<i>IL13</i>	2.00E-18	134.27	7.069	7	<i>TMEM38A</i>	8.94E-07	-4.47	-2.16
8	<i>AL353608.3</i>	0.000397	94.03	6.555	8	<i>ADRA2A</i>	2.01E-10	-4.29	-2.10
9	<i>AC007336.2</i>	4.08E-06	82.54	6.367	9	<i>AC019197.1</i>	0.002786	-4.23	-2.08
10	<i>TNF</i>	9.71E-16	80.34	6.328	10	<i>PLXNA4</i>	1.42E-09	-4.18	-2.06
11	<i>C3</i>	1.19E-18	67.23	6.071	11	<i>ANGPT2</i>	2.91E-15	-4.16	-2.06
12	<i>AC083837.1</i>	2.28E-19	62.90	5.975	12	<i>SCN3A</i>	2.40E-08	-4.16	-2.06
13	<i>MFAP5</i>	2.71E-05	60.59	5.921	13	<i>ZBTB16</i>	1.43E-08	-4.09	-2.03
14	<i>CSF3</i>	0.003747	59.26	5.889	14	<i>GDF2</i>	9.69E-14	-4.08	-2.03
15	<i>TNFAIP2</i>	3.13E-21	56.45	5.819	15	<i>SHE</i>	0.000257	-4.01	-2.00
16	<i>ITGA1</i>	1.38E-18	55.33	5.79	16	<i>RSPO2</i>	4.44E-07	-3.96	-1.99
17	<i>BCL2A1</i>	5.41E-16	46.11	5.527	17	<i>NFE2</i>	5.33E-13	-3.87	-1.95
18	<i>SERPINE1</i>	1.74E-14	38.67	5.273	18	<i>GIPC3</i>	0.031608	-3.74	-1.90
19	<i>LRFN5</i>	4.34E-12	37.37	5.224	19	<i>COBLL1</i>	1.38E-09	-3.67	-1.88
20	<i>CXCL10</i>	1.79E-06	35.31	5.142	20	<i>PTPN5</i>	1.19E-18	-3.68	-1.88
21	<i>NINJ1</i>	1.73E-23	34.94	5.127	21	<i>AC092155.1</i>	0.002428	-3.65	-1.87
22	<i>PDZD2</i>	1.35E-20	32.72	5.032	22	<i>AL670729.3</i>	4.71E-07	-3.63	-1.86
23	<i>SECTM1</i>	1.01E-12	30.25	4.919	23	<i>LINC01366</i>	4.59E-12	-3.63	-1.86
24	<i>TSPAN18</i>	7.29E-11	29.10	4.863	24	<i>CTPS2</i>	4.16E-05	-3.63	-1.86
25	<i>CXCL8</i>	9.57E-14	29.02	4.859	25	<i>DACH1</i>	7.09E-09	-3.58	-1.84
26	<i>TMEM132E</i>	1.76E-09	28.76	4.846	26	<i>FEV</i>	0.114045	-3.59	-1.84
27	<i>TRABD2B</i>	3.02E-09	28.74	4.845	27	<i>DMTN</i>	1.26E-05	-3.55	-1.83
28	<i>PTGIR</i>	5.22E-13	28.01	4.808	28	<i>UNC80</i>	1.88E-07	-3.55	-1.83
29	<i>GBP5</i>	4.11E-14	26.87	4.748	29	<i>CXXC4</i>	1.32E-05	-3.53	-1.82
30	<i>ACAN</i>	5.12E-08	26.21	4.712	30	<i>PTGDR2</i>	6.14E-06	-3.51	-1.81
31	<i>ROR1-AS1</i>	5.11E-14	24.92	4.639	31	<i>SEC14L5</i>	1.00E-12	-3.40	-1.76
32	<i>NFKBIA</i>	6.54E-17	22.16	4.47	32	<i>CEBPA</i>	2.50E-05	-3.40	-1.77
33	<i>IL5</i>	1.67E-07	21.92	4.454	33	<i>NPY2R</i>	1.38E-09	-3.34	-1.74
34	<i>PTP4A3</i>	2.09E-14	21.60	4.433	34	<i>EDNRB</i>	4.65E-11	-3.33	-1.74
35	<i>AC010247.1</i>	6.07E-16	21.53	4.428	35	<i>MEX3B</i>	1.15E-14	-3.31	-1.73
36	<i>N4BP3</i>	1.53E-15	21.21	4.407	36	<i>CEBPE</i>	4.12E-08	-3.27	-1.71
37	<i>AC083864.5</i>	1.45E-10	20.84	4.381	37	<i>RD3</i>	5.62E-15	-3.27	-1.71
38	<i>IL1B</i>	9.34E-07	20.72	4.373	38	<i>AC097713.1</i>	0.007003	-3.27	-1.71
39	<i>TNFRSF9</i>	1.73E-23	20.72	4.373	39	<i>A4GALT</i>	5.74E-05	-3.22	-1.69

40	<i>GFPT2</i>	1.37E-14	20.72	4.373
41	<b><i>TLR7</i></b>	<b>3.83E-10</b>	<b>20.14</b>	<b>4.332</b>
42	<i>CXCL3</i>	5.07E-11	20.06	4.326
43	<i>CCL3L3</i>	6.88E-18	19.64	4.296
44	<i>VSTM2A</i>	5.12E-07	19.20	4.263
45	<i>TRAF1</i>	4.70E-27	18.97	4.246
46	<i>MMP10</i>	3.04E-07	18.83	4.235
47	<i>IL2RA</i>	8.18E-17	18.58	4.216
48	<i>POU2F2</i>	4.64E-27	18.46	4.206
49	<i>LINC01215</i>	7.97E-17	18.46	4.206
50	<i>TSLP</i>	0.001398	17.68	4.144

40	<i>GXYLT1P6</i>	6.35E-08	-3.18	-1.67
41	<i>PTCH1</i>	5.85E-11	-3.16	-1.66
42	<i>HEMGN</i>	0.014634	-3.16	-1.66
43	<i>JPH4</i>	1.37E-16	-3.14	-1.65
44	<i>CLK3P2</i>	2.61E-08	-3.12	-1.64
45	<i>PADI2</i>	3.17E-10	-3.08	-1.63
46	<i>CNNM1</i>	0.028685	-3.09	-1.63
47	<i>GPAT3</i>	1.25E-12	-3.08	-1.62
48	<i>RAB6C-AS1</i>	0.000126	-3.06	-1.62
49	<i>TOGARAM2</i>	1.27E-05	-3.07	-1.62
50	<i>CRISPLD2</i>	0.000138	-3.00	-1.58

598

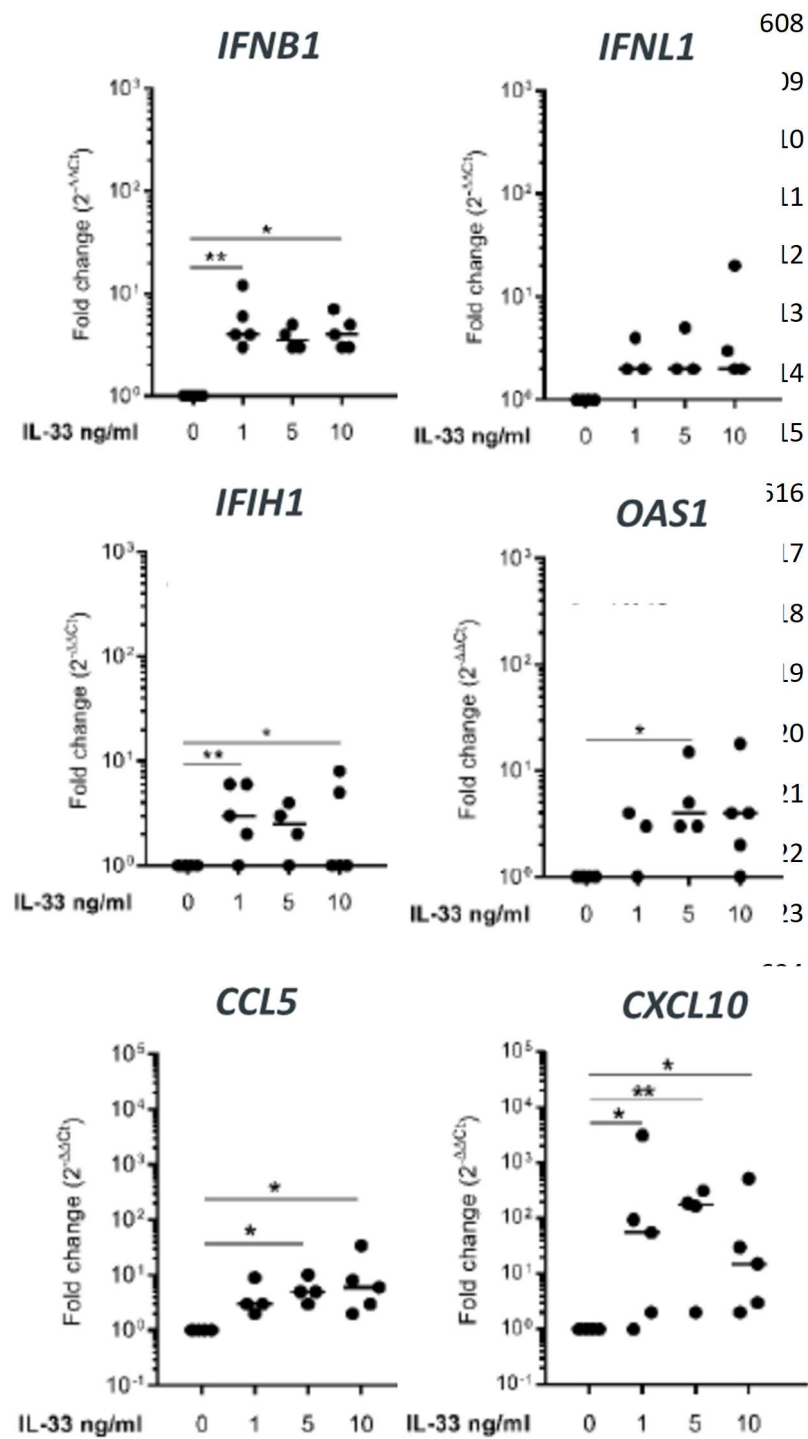
599 **Figure S1:** Violin plots of antiviral genes associated with HRV infection in LAD2 MCs. From the  
 600 transcriptomic data the significant DEGs associated with HRV infection of BECs were identified in the  
 601 LAD2 MC + IL-33 (10 ng/ml) dataset and replicate samples displayed as violin plots for control (green)  
 602 and IL-33 (blue) treated samples, n=7.



603

604 **Figure S2:** Concentration-dependent induction of IFN and IFN-inducible genes by IL-33 in MCs.  
605 Validation of *IFNB1*, *IFNL1*, *IFIH1*, *OAS1*, *CCL5* and *CXCL10* gene induction by IL-33 (1, 5, 10  
606 ng/ml) treatment for 24h, n=5.

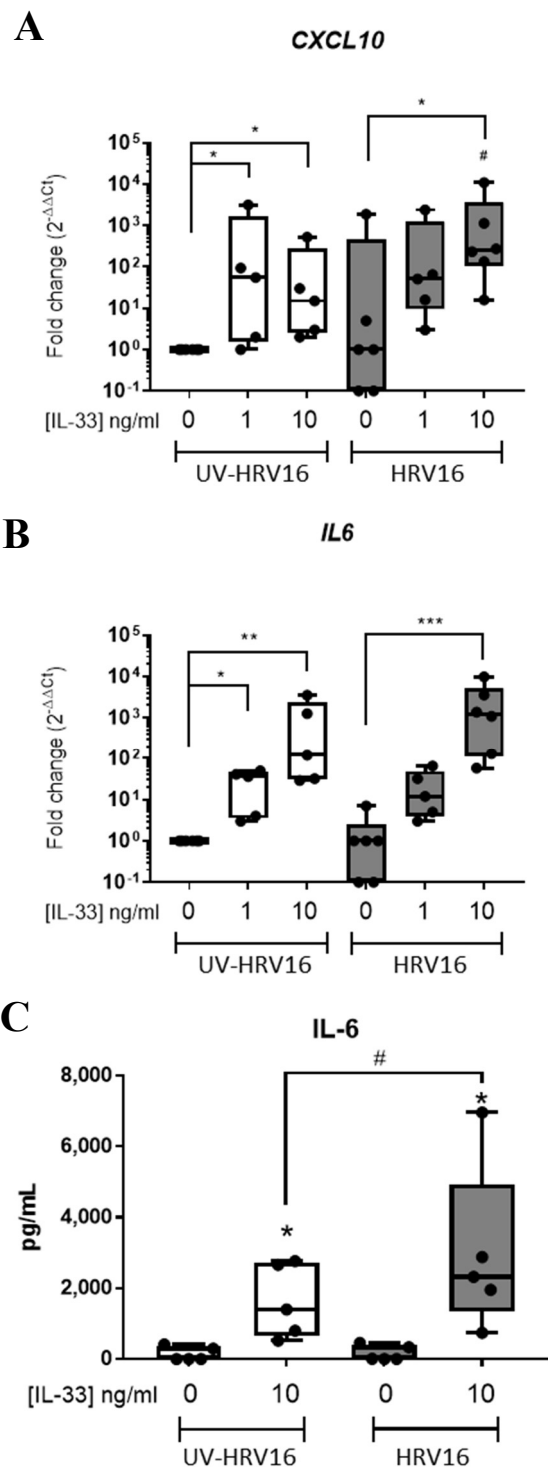
607



633

634 **Figure S3:** HRV16 affects IL-33-dependent CXCL10 and IL6 release. mRNA expression of *CXCL10*  
635 (A) and *IL6* (B) and IL6 protein (C) in LAD2 MCs pretreated with or without IL-33 (1-10 ng/ml) for  
636 24h prior to HRV16 or UV-HRV16 (control) infection (MOI 7.5) for a further 24h, n=5-6.

637

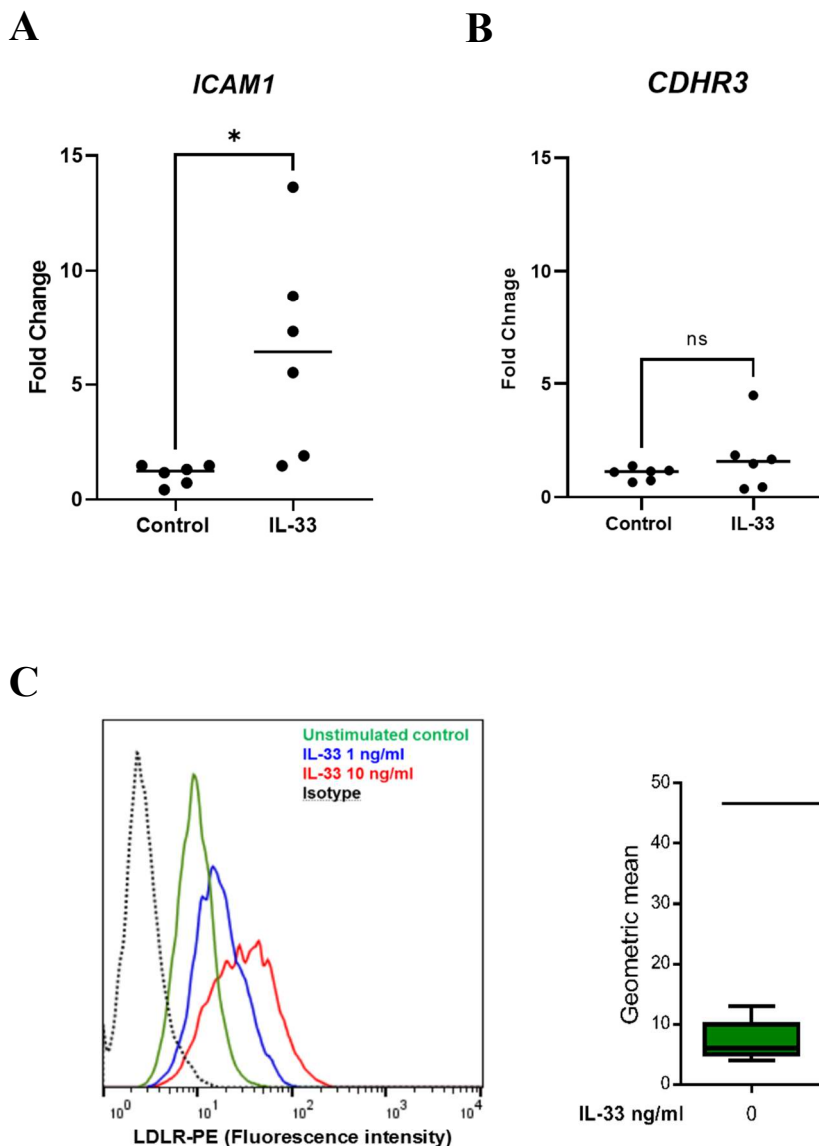


638

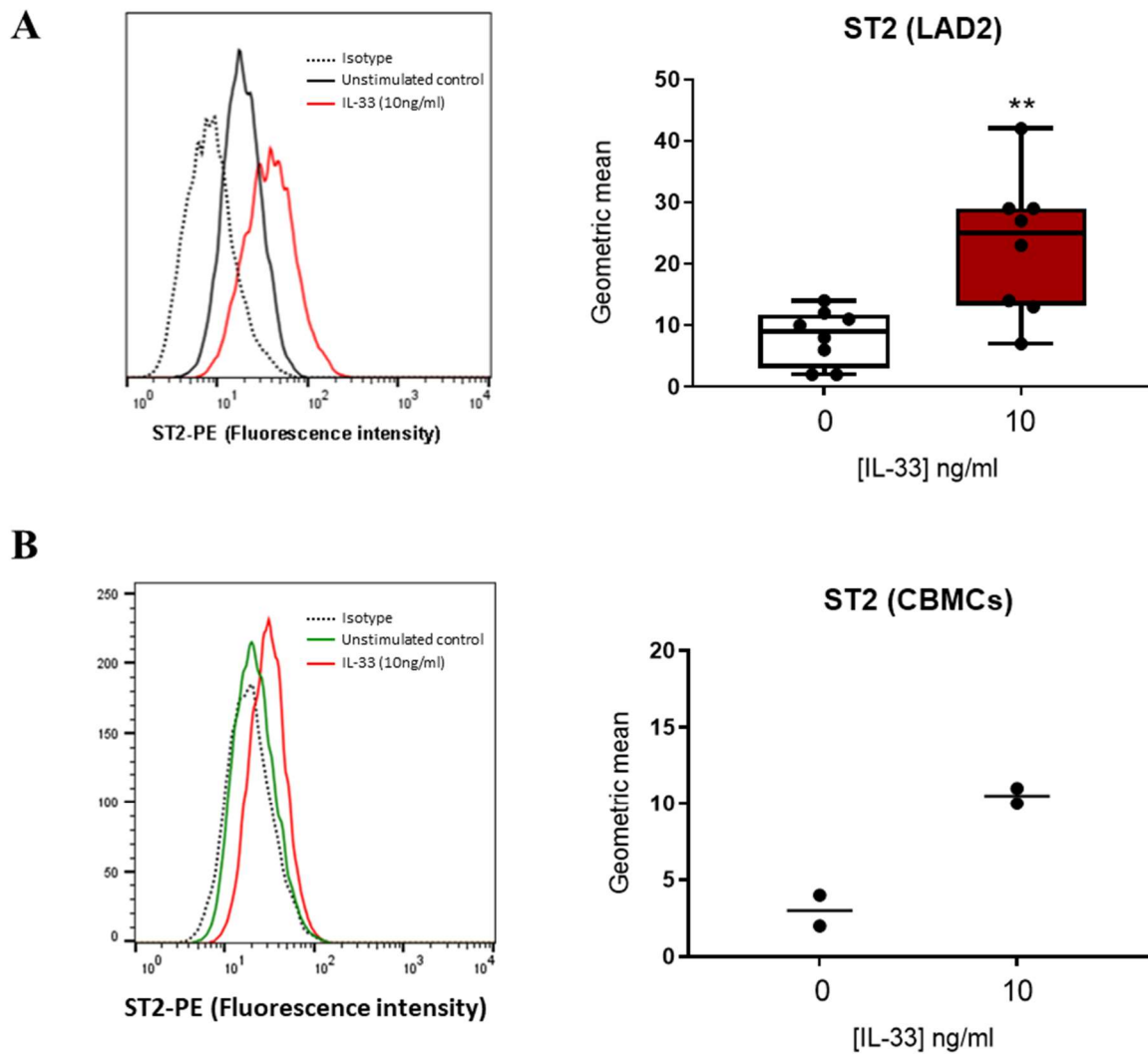
639

640 **Figure S4:** IL-33 enhances ICAM1, LDLR but not CDHR3. *ICAM1* (A) and *CDHR3* (B) gene  
641 expression in MCs treated with IL-33 (10 ng/ml) for 24h, n=6. LDLR (C) cell surface expression in  
642 MCs treated with IL-33 (10 ng/ml) for 24h, n=4-7.

643



663 **Figure S5:** IL-33 enhances membrane ST2 in LAD2 MCs and CBMCs. **A**, ST2 cell surface expression  
664 in LAD2 MCs treated with IL-33 (10 ng/ml) for 24h, n=8. **B**, ST2 cell surface expression in CBMCs  
665 treated with IL-33 (10 ng/ml) for 24h, n=2.



666

667

668 **Supplementary File S2: Supplemental Materials and Methods**

669 *2.1. Mast cell culture*

670 The human MC line, LAD2, was obtained from Dr. A. Kirshenbaum (National  
671 Institutes of Health, Bethesda, USA) [43] and was cultured in Stem Pro-34® serum-free basal  
672 medium (Gibco, ThermoFisher, Paisley, UK) supplemented with 2-mM L-glutamine, 100  
673 IU/ml penicillin, 100 µg/ml streptomycin, and 100 ng/ml recombinant stem cell factor (SCF)  
674 (Peprotech, UK), as previously described [23]. Primary cord blood-derived MCs (CBMCs)  
675 were generated as previously described [23] from a commercial source of CD34+ cord blood  
676 progenitor cells (StemCell technologies, Grenoble, France). Briefly, CD34+ cells were cultured  
677 in StemPro® medium supplemented with 2 mM L-glutamine, 100 IU/ml penicillin, 100 µg/ml  
678 streptomycin, IL-3 (30 ng/ml, 1 week only, Peprotech, UK), IL-6 (100 ng/ml, Peprotech, UK)  
679 and SCF (100 ng/ml) for 3 weeks by hemidepletion before culture media was completely  
680 replaced weekly thereafter. After 8-10 weeks, CBMCs were assessed for purity by FcεRI and  
681 CD117 expression by flow cytometry

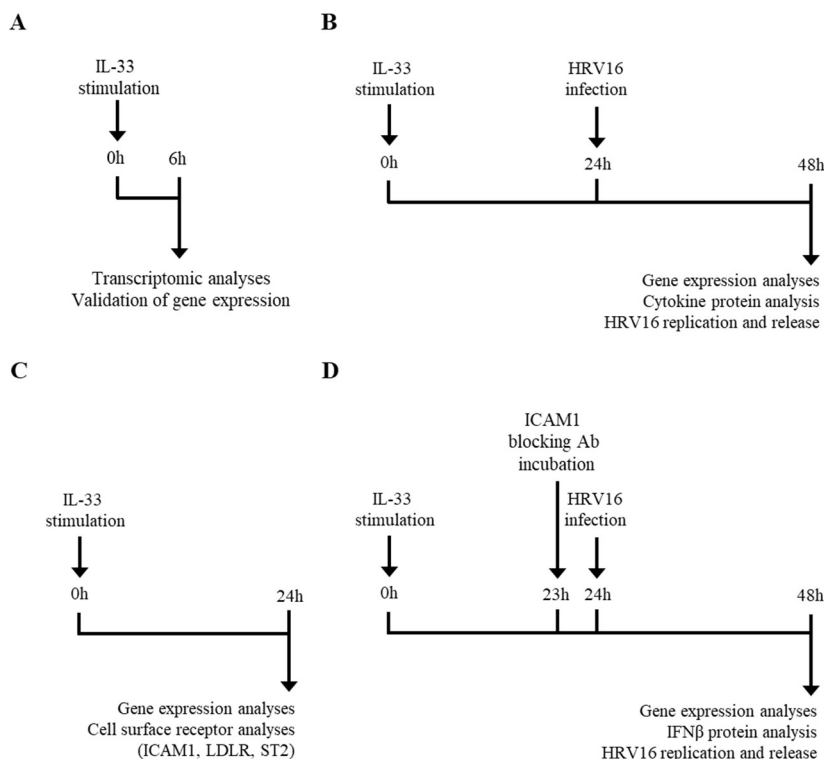
682 *2.2. Rhinovirus stocks*

683 Human rhinovirus serotype 16 (HRV16, major group, HRV-B species) stocks were  
684 generated using H1-HeLa cells obtained from ATCC as previously described [23]. Virus titres  
685 of cell-free supernatant stocks were determined by tissue culture infective dose 50%  
686 (TCID<sub>50</sub>)/mL according to the Spearman-Karber method. Controls of UV-irradiated HRV16  
687 (1,200 mJ/cm<sup>2</sup> on ice for 50 min) were included in all experiments.

688 *2.3. Cell treatments and infections*

689 Human MCs (1x10<sup>6</sup>/ml) were incubated with IL-33 (1-10 ng/ml, R&D Systems,  
690 Abingdon, UK) for 6-24 hours in a humidified 37°C incubator with 5% CO<sub>2</sub> before  
691 transcriptomic and qPCR analysis. For RV16 infection, the LAD2 cell line or CBMCs were

692 incubated with increasing MOI (1 – 7.5) of infectious virus or UV-irradiated virus (as a control)  
 693 for 1 hour whilst rocking in the dark at 36 opm. Cells were then washed twice to remove  
 694 unbound virus, resuspended in StemPro media ( $0.5\text{-}1\times 10^6/\text{ml}$ ) and incubated for 24 hours in a  
 695 humidified  $37^\circ\text{C}$  incubator with 5%  $\text{CO}_2$  before harvesting. For ICAM-1 blocking experiments,  
 696 LAD2 MCs or CBMCs ( $1\times 10^6/\text{ml}$ ) were treated with 10 ng/ml IL-33 for 23 hours followed by  
 697 1 hour with mouse anti-human ICAM-1 (clone BBIG-I1 (11C81), 10  $\mu\text{g}/\text{ml}$ , R&D Systems,  
 698 Abingdon, UK) or IgG2a isotype control (10  $\mu\text{g}/\text{ml}$ , R&D Systems, Abingdon, UK). Following  
 699 HRV16 infection of MCs, the antibodies were re-introduced and cultures incubated for a  
 700 further 24 hours. Experimental layouts are shown below (Figure B1).



701

702 **Figure A:** Experimental layout of stimulations of MCs with IL-33 and HRV16. LAD2 MCs were  
 703 treated for 6h with IL-33 (10 ng/ml) prior to transcriptomic analyses (A, Figures 1-2, A1, Table A1)  
 704 whereas LAD2 or CBMCs were treated with IL-33 for 24h prior to HRV16 infection and samples  
 705 collected 24h later for gene expression, IFN-beta protein release, HRV16 replication and release (B,  
 706 Figures 3-4, 6A, A2-A3). For cell surface receptor analyses by RT-qPCR and flow cytometry (ICAM1,  
 707 LDLR, ST2), LAD2 MCs or CBMCs were stimulated with IL-33 (10 ng/ml) for 24h prior to analyses  
 708 (C, Figure 5A-B, 6B-C, A4-A5). Where an ICAM1 blocking antibody was used, the blocking antibody  
 709 (Ab) was added to LAD2 MC or CBMCs 23h post-IL-33 stimulation for 1h before infection with  
 710 HRV16. Samples were then collected 24h post-HRV16 infection (D, Figure 5C-E, 6D-F).

711 2.4. mRNA extraction, RNA sequencing and transcriptomic analysis

712 The LAD2 MC line was incubated with IL-33 (10 ng/ml) or media control for 6 hours  
713 in StemPro® media containing SCF (100 ng/ml). Total RNA was isolated using either the Trizol  
714 extraction method as previously described [23] or using commercially available kits (RNeasy  
715 minikit, Qiagen (Manchester, UK) or Monarch total RNA miniprep kit (New England Biolabs,  
716 Hitchin, UK)) and quantified for RNA quantity and quality (Nanodrop, ThermoFisher, Paisley,  
717 UK). Next generation sequencing was performed by Novogene (Cambridge, UK) at a read  
718 depth of 20 million reads per sample following quality control checks and data pre-processing.  
719 Raw reads were stored as FASTQ files, uploaded to the Iridis computer cluster (University of  
720 Southampton), mapped to the human genome (HISAT2), annotated with gene names and  
721 converted to counts (SAMtools). Using RStudio, the count matrix was then adjusted for batch  
722 effects (ComBat Seq within sva package) before low counts were filtered out (EdgER) and  
723 those remaining were normalised using a weighted trimmed mean of the log expression ratios  
724 (trimmed mean of M values (TMM)). The resultant expression matrix was used to create  
725 Multidimensional scaling plots (limma, Rstudio) and Heatmaps (heatmap.2, RStudio) and a  
726 fitted to a generalised linear model (quasi-likelihood F-test) for differential expression.  
727 Volcano plots were generated of all detected genes (EnhancedVolcano package, RStudio).  
728 Differentially expressed genes (DEGs) were defined as genes with a  $\log_2$ (fold change)  
729 ( $\log_2FC$ ) $>1.5$  and a False Discovery Rate (FDR)-adjusted p value  $<0.05$ . The significantly  
730 upregulated genes were inputted into g:profiler (<https://biit.cs.ut.ee/gprofiler/gost>) with the  
731 background gene set to the total human genome and term size limited (5 -10,000) for Gene  
732 ontology (GO) and pathways analysis (KEGG). The resulting GO terms were then submitted  
733 to REVIGO for visualisation and gene set enrichment analysis (GSEA). Data are available at  
734 GSE2162692.5. RT-qPCR

735 Isolated RNA was DNase I treated (Stemcell Technologies, Cambridge, UK), reverse  
736 transcribed to cDNA using precision nanoScript2 reverse transcription kit (PrimerDesign,  
737 Chandlers Ford, UK) and 12.5 ng used as a template in quantitative PCR (qPCR) with Precision  
738 Plus double dye primers for housekeeping genes (HKGs; *GAPDH*, *UBC*) or genes of interest  
739 (*IFIH1*, *IRF1*, *TNFA*, *IFNB1*, *IFNL1*, *MDA5*, *OASI*, *CXCL10*, *IL6*, *CCL5*) or SYBR® green  
740 primers for genes of interest (*ICAM1*) used to quantify amplification of genes. All reactions  
741 were performed in duplicate for 50 cycles and gene expression analysed using a real-time PCR  
742 iCycler (BioRad, Hemel Hempstead, UK). For SYBR green detection-based reactions, melt  
743 curves were performed to ensure single PCR product formation. Gene expression was  
744 normalised to the geometric means of HKGs and fold changes in gene expression calculated  
745 relative to UV-HRV16 controls according to the  $\Delta\Delta Ct$  method and expressed as  $2^{-\Delta\Delta Ct}$ . Viral  
746 RNA copy number was determined against a standard curve of known copies of HRV16  
747 (Primerdesign, Chandlers Ford, UK).

748 2.6. *Flow cytometry*

749 Human MCs were washed with FACS buffer (PBS + 0.5% (v/v) BSA + 2 mM EDTA)  
750 prior to blocking with block buffer (PBS + 10% (v/v) heat inactivated human serum + 2 mM  
751 EDTA) for 20 minutes on ice. Cells ( $0.1 \times 10^6$ /100  $\mu$ l) were then incubated with fluorescently  
752 labelled antibodies, FITC-conjugated mouse anti-human ICAM1 (clone RR1/1), subclass  
753 IgG<sub>1</sub>) or mouse IgG<sub>1</sub> isotype control (eBiosciences, Cheshire, UK) for 30 minutes with the  
754 addition of eBioscience™ Fixable Viability Dye eFluor™ 660 (Thermo Fisher Scientific,  
755 Paisley, UK) on ice prior to washing and resuspending in 300  $\mu$ l FACS buffer. At least 10,000  
756 events were collected for analysis and gating was performed on non-APC expressing cells, i.e.  
757 live cells, and ICAM1 geometric means expressed minus that of isotype controls. Flow  
758 cytometry was performed using a BD FACSCalibur flow cytometer (BD Biosciences, Oxford,  
759 UK) and data analysed using FlowJo software (version 7.6.5, BD, Oregon, USA).

760 2.7. *TCID<sub>50</sub> assay*

761 The number of infectious virus particles in cell-free supernatants was determined by  
762 the TCID<sub>50</sub> assay where a 10-fold serial dilution of supernatants in quadruplicate were added  
763 to OHIO HeLa cells ( $0.2 \times 10^6$ /well, 96-well plate). After 96 hours, cytopathic effect (CPE) was  
764 visualised by staining monolayers with crystal violet solution (0.13% (w/v), 1.825% (v/v)  
765 formaldehyde, 5% ethanol (v/v), 90% PBS (v/v) for 30 minutes in the dark. Excess crystal  
766 violet was removed by gentle rinsing and the number of wells where at least 50% of the  
767 monolayer had been lysed (i.e. 50% CPE) was used to calculate TCID<sub>50</sub>/ml using the  
768 Spearman-Karber Method

769 2.8. *Statistical analysis*

770 Paired non-parametric data were analysed by Wilcoxon signed rank test for matched  
771 pair comparisons. Un-paired non-parametric data were analysed by Kruskal–Wallis one-way  
772 ANOVA with Dunn's correction for multiple comparisons or Mann–Whitney ranked sum test  
773 and normalised data were analysed by Student's t-test. All data were analysed using GraphPad  
774 Prism (GraphPad Software, Inc., San Diego, CA, USA).

775

776